SIAM J. NUMER. ANAL.
Vol. 32, No. 4, pp. 1017-1057, August 1995

PROJECTION METHOD I: CONVERGENCE AND NUMERICAL BOUNDARY LAYERS*

WEINAN E† AND JIAN-GUO LIU‡

Abstract. This is the first of a series of papers on the subject of projection methods for viscous incompressible flow calculations. The purpose of these papers is to provide a thorough understanding of the numerical phenomena involved in the projection methods, particularly when boundaries are present, and point to ways of designing more efficient, robust, and accurate numerical methods based on the primitive variable formulation. This paper contains the following topics:

1. convergence and optimal error estimates for both velocity and pressure up to the boundary;
2. explicit characterization of the numerical boundary layers in the pressure approximations and the intermediate velocity fields;
3. the effect of choosing different numerical boundary conditions at the projection step. We will show that a different choice of boundary conditions gives rise to different boundary layer structures. In particular, the straightforward Dirichlet boundary condition for the pressure leads to $O(1)$ numerical boundary layers in the pressure and deteriorates the accuracy in the interior; and
4. postprocessing the numerical solutions to get more accurate approximations for the pressure.

Key words. viscous incompressible flows, projection method, convergence, numerical boundary layers

AMS subject classifications. 65M06, 76M20

1. Introduction. The projection method was introduced years ago in a series of papers by Chorin [5]–[7] as a way of computing efficiently the solutions of incompressible Navier–Stokes equations (NSE). Similar ideas can also be found in the papers of Temam [25]. The method is getting increasingly popular in applications to viscous incompressible flows at a moderate Reynolds number. With periodic boundary conditions, the performance of the projection method is well understood from the work of Chorin [7]. Much less is known when physical boundary conditions such as the no-slip boundary conditions are used, although convergence was already proved in [7]. It has been a mystery for twenty-five years that the projection method seems to perform better than expected. There are still controversies with regard to the optimal choice of boundary conditions at the projection step. Furthermore, although it is clear that numerical boundary layers must be present, little is known about their structures.

It is the purpose of this series of papers to fully clarify these issues. Besides being able to answer all these questions, we find that the effect of solid boundaries is not restricted to creating numerical boundary layers; they can also give rise to high-frequency oscillations in the leading-order error term, reducing the order of accuracy even in the *interior* of the domain [9]. But when formulated appropriately, the projection method is indeed an efficient numerical procedure for viscous incompressible flow calculations. Before our work, comparison of different formulations of the projection method was only possible through careful numerical experiments. These numerical experiments are made difficult by the fact that in actual computations, the effect of temporal and spatial discretizations, as well as the numerical boundary

* Received by the editors November 23, 1992; accepted for publication January 27, 1994.

† School of Mathematics, Institute for Advanced Study, Princeton, New Jersey 08540 (weinan@math.ias.edu). The work of the author was supported in part by National Science Foundation grant DMS-86-10730.

‡ Courant Institute of Mathematical Sciences, New York, New York 10012 (jliu@cims.nyu.edu). The work of this author was supported in part by National Science Foundation grant DMS-9114456 and Department of Energy grant DE-FG02-88ER25053.

conditions, are all mixed together. Moreover, they usually involve a systematic study of two-dimensional problems for which the resolution power of modern computers is still quite limited. In our work, we have developed procedures for studying separately the effect of different components of the projection method. In forthcoming papers, we will also make extensive use of one-dimensional models which capture much of the *computational* difficulties for incompressible flow calculations.

The present paper is devoted to the explicit characterization of the numerical boundary layers. As a consequence, we also get optimal convergence and error estimates for both velocity and pressure up to the boundary. The boundary layer structure is strongly influenced by the numerical boundary condition for pressure at the projection step. We will study different choices of the pressure boundary conditions and compare their performance in terms of the accuracy of the numerical solutions. Our analysis favors strongly the choice of Neumann boundary conditions.

Roughly speaking, the projection method was based on the following philosophy: In incompressible flows, pressure does not carry any thermodynamic meaning and is present only as a Lagrange multiplier for the incompressibility constraint [6]. This observation motivated a time-splitting discretization scheme which decouples the computation of velocity and pressure, a key feature of the projection method. In the first step, an intermediate velocity field is computed using the momentum equation and ignoring the incompressibility constraint. In the second step, the intermediate velocity is projected to the space of divergence-free vector fields to get the next update of velocity and pressure. This procedure is much more efficient than solving a coupled system of Stokes equations for velocity and pressure which would arise from a straightforward time discretization of the NSE (see §2). The price that has been paid, as we will see below, is that it introduces a numerical boundary layer on the pressure approximations and the intermediate velocity fields. This also signifies the main difficulty in the design and implementation of more efficient projection methods: treatment of the boundary conditions.

Over the years the projection method has played a dominant role in the computation of viscous incompressible flows based on the primitive variable formulation. It has also acquired other names such as the splitting scheme, fractional step method, etc. Recently there has been a flourish of interest in the application of projection methods for the direct simulation of viscous incompressible flows at moderate Reynolds numbers [3], [4], [15], [16], [20], [28], etc. Notable in these applications are the various spatial discretizations used, including flux (slope)-limited finite difference methods [3], [4], upwind differencing [20], and spectral-element methods [15].

The analysis of the projection methods was also initiated by Chorin and Temam. In the case of periodic boundary conditions Chorin proved the convergence of a projection method which uses a backward Euler in time and centered differencing in space. His analysis can be easily extended to other methods of a similar nature as long as the periodic boundary condition is retained. Chorin's analysis was facilitated by the fact that with periodic boundary conditions, the projection operator and the laplacian commute. This no longer holds for other types of boundary conditions. As a result, it is much more difficult to study the projection methods when the boundary condition is changed to more physical ones such as the no-slip condition, especially when it comes to the issue of accuracy. Indeed a crude analysis indicates that there is a real danger that the numerical boundary layer in pressure could pollute the numerical solutions in the interior and significantly reduce the overall accuracy (even for velocity) [3], [7], although numerical evidence seems to indicate otherwise. For more recent results on the analysis of the projection method, we refer to [21]–[23]. Some of the results in [22], [23] were disputed in [13]. Related work on the analysis of the Euler–Stokes splitting procedure can be found in [2].

One result of this paper is a proof that the numerical approximation of velocity indeed has the maximum accuracy. The proof is based on a systematic asymptotic analysis of the numerical solutions. The numerical method is viewed as a singular perturbation of the original NSE, and boundary layer analysis is used to construct approximate solutions which satisfy the numerical scheme to high-order accuracy. This, plus the linear stability of the scheme, implies the convergence results. This line of thought is often used in applied analysis and was first used by Strang [24] in the context of numerical analysis, although Strang only dealt with a regular perturbation problem. By using similar ideas, Michelson [17] extended Strang's argument to initial-boundary value problems for hyperbolic systems.

The advantage of this approach is that the numerical boundary layers are explicitly characterized. This enables us to propose simple ways of removing the numerical boundary layer by postprocessing the numerical solutions. The disadvantage, however, is that it requires far more regularity of the exact solutions than necessary. This translates to a Reynolds number dependence of the error estimates that is far from being optimal. This is an important issue since very often in actual computations, the smallest mesh size is set by the memory of the machine, and the issue is to resolve flows with the largest possible Reynolds number. In the second paper of this series [9], we will give an entirely different proof based on Godunov–Ryabenki analysis which not only gives the optimal convergence results with minimum assumptions, but also exhibits clearly the effect of noncommutativity of the various operators involved.

For convenience, we list here the content of the rest of the paper: §2 review of the projection methods, §3 summary of results and outline of proofs, §4 first-order schemes without spatial discretization, §5 effect of numerical boundary conditions, §6 second-order schemes without spatial discretization, §7 generalizations, and in the Appendix, postprocessing for the pressure.

2. Review of the projection methods. In primitive variables, NSE takes the following form

$$\left\{ \begin{array}{l} \partial_t \boldsymbol{u} + (\boldsymbol{u}\cdot\nabla)\boldsymbol{u} + \nabla p = \Delta \boldsymbol{u}\,, \\ \nabla\cdot\boldsymbol{u} = 0\,. \end{array} \right. \tag{2.1}$$

Here $\boldsymbol{u} = (u, v)$ is the velocity, and p is the pressure. For simplicity, we will only consider the case when the no-slip boundary condition is supplemented to (2.1):

$$\boldsymbol{u} = 0 \qquad \text{on } \partial\Omega, \tag{2.2}$$

where Ω is an open domain in $\boldsymbol{R}^2$ with a smooth or piecewise smooth boundary.

2.1. Time discretization. As a first step toward the construction of an efficient numerical scheme for (2.1)–(2.2), we discretize (2.1) in time using backward Euler methods:

$$\left\{ \begin{array}{l} \dfrac{\boldsymbol{u}^{n+1} - \boldsymbol{u}^n}{\Delta t} + (\boldsymbol{u}^n\cdot\nabla)\boldsymbol{u}^n + \nabla p^{n+1} = \Delta \boldsymbol{u}^{n+1}\,, \\ \nabla\cdot\boldsymbol{u}^{n+1} = 0\,. \end{array} \right. \tag{2.3}$$

We do not hesitate to use implicit schemes since the NSE is intrinsically implicit anyway. Alternatively we can discretize (2.1) using the trapezoidal rule, resulting in the Crank–Nicholson scheme:

$$\begin{cases} \dfrac{\boldsymbol{u}^{n+1}-\boldsymbol{u}^n}{\Delta t}+(\boldsymbol{u}^{n+1/2}\cdot\nabla)\boldsymbol{u}^{n+1/2}+\nabla p^{n+1}=\Delta\dfrac{\boldsymbol{u}^{n+1}+\boldsymbol{u}^n}{2}\,, \\ \nabla\cdot\boldsymbol{u}^{n+1}=0\,. \end{cases} \tag{2.4}$$

It is not important at this point to specify the discretization for the convection terms. (2.3) and (2.4) are solved together with the boundary condition:

$$\boldsymbol{u}^{n+1}=0 \qquad \text{on } \partial\Omega\,. \tag{2.5}$$

However, both schemes are highly inefficient since they require, at each time step, the solution of (2.3) or (2.4) which are coupled systems of Stokes-like equations for $(\boldsymbol{u}^{n+1}, p^{n+1})$. This is precisely the reason for proposing the projection method as a numerical device to decouple the computation of $\boldsymbol{u}^{n+1}$ and p^{n+1} [5]. Instead of simultaneously satisfying the momentum equation and the incompressibility constraint, the projection method proceeds by first ignoring the incompressibility constraint, computing an intermediate velocity field $\boldsymbol{u}^*$ using the momentum equation, and then projecting $\boldsymbol{u}^*$ back to the space of incompressible vector fields to obtain $\boldsymbol{u}^{n+1}$ and p^{n+1}. The actual realization of this procedure for the first-order scheme can be summarized as the following.

First-order scheme.

Step 1.

$$\begin{cases} \dfrac{\boldsymbol{u}^*-\boldsymbol{u}^n}{\Delta t}+(\boldsymbol{u}^n\cdot\nabla)\boldsymbol{u}^n=\Delta\boldsymbol{u}^*, \\ \boldsymbol{u}^*=0 \qquad \text{on } \partial\Omega. \end{cases} \tag{2.6}$$

Step 2.

$$\begin{cases} \boldsymbol{u}^*=\boldsymbol{u}^{n+1}+\Delta t\nabla p^{n+1}, \\ \nabla\cdot\boldsymbol{u}^{n+1}=0. \end{cases} \tag{2.7}$$

The boundary condition for $\boldsymbol{u}^*$ in (2.6) is rather natural, at least for the first-order scheme. The agonizing decision to be made is the boundary condition for (2.7). If we take the inner product of (2.1) with the unit normal and tangent vectors at $\partial\Omega$, $\boldsymbol{n}$, and $\boldsymbol{t}$, respectively, we arrive at

$$\frac{\partial p}{\partial \boldsymbol{n}}=\boldsymbol{n}\cdot\Delta\boldsymbol{u}\,, \qquad \frac{\partial p}{\partial \boldsymbol{t}}=\boldsymbol{t}\cdot\Delta\boldsymbol{u} \qquad \text{on } \partial\Omega\,. \tag{2.8}$$

So both the Neumann and Dirichlet boundary conditions seem plausible for the pressure in (2.7). The prevailing point of view for resolving this ambiguity is the following [8]. The boundary condition in (2.7) is part of the specification of the projection operator. If one requires that the space of divergence-free vector fields be orthogonal (with respect to the usual L^2 inner product) to the space of irrotational vector fields, then the divergence-free fields have to satisfy the boundary condition:

$$\boldsymbol{u}\cdot\boldsymbol{n}=0 \qquad \text{on } \partial\Omega\,. \tag{2.9}$$

Therefore for (2.7) one has

$$u^{n+1}\cdot n = 0\,, \quad \text{or} \quad \frac{\partial p^{n+1}}{\partial n} = 0\,, \qquad \text{on } \partial\Omega\,. \tag{2.10}$$

In this case (2.7) is none other than the standard Helmholtz decomposition. This boundary condition is strongly favored in the literature. The question to be addressed then is whether orthogonality is really important.[1]

The bottom line is that in most situations, large errors will be introduced at the boundary, either on velocity or on pressure, because of the inconsistency of the boundary conditions. The hope is that these large errors will be restricted to a boundary layer and not affect the accuracy in the interior. Whether this actually happens is precisely the question to be addressed here.

To give an indication that the numerical solution contains boundary layers, let us consider the linear case. Without the nonlinear term, (2.6), (2.7), and (2.10) combine to give

$$\begin{cases} (I - \Delta t\Delta)\Delta p^{n+1} = 0\,, \\ \dfrac{\partial p^{n+1}}{\partial n} = 0 \qquad \text{on } \partial\Omega\,. \end{cases} \tag{2.11}$$

In contrast, the linear Stokes equations imply

$$\Delta p = 0$$

without boundary condition on p. Therefore if $p^{n+1}(x)$ has any chance of being close to $p(x,(n+1)\Delta t)$, there must be numerical boundary layers in p^{n+1} with thickness $O(\Delta t^{1/2})$. This is indeed the case as will be seen in §§3 and 4.

Second-order schemes. There are at least three different ways to decouple the system (2.4) to get a formally second-order scheme. These are, respectively, projection methods based on (1) accurate boundary conditions for the intermediate velocity field [16]; (2) accurate pressure boundary conditions [19]; (3) pressure increment formulation [3], [28]. Below is a summary of these methods.

(1) Projection method based on accurate boundary conditions for the intermediate velocity field (Kim and Moin's method [16]):

$$\begin{cases} \dfrac{u^* - u^n}{\Delta t} + (u^{n+1/2}\cdot\nabla)u^{n+1/2} = \Delta\dfrac{u^* + u^n}{2}\,, \\ u^* + u^n = \Delta t\nabla p^{n-1/2} \qquad \text{on } \partial\Omega\,, \\ u^* = u^{n+1} + \Delta t\nabla p^{n+1/2}\,, \\ \nabla\cdot u^{n+1} = 0\,, \\ n\cdot u^{n+1} = 0 \qquad \text{on } \partial\Omega\,. \end{cases} \tag{2.12}$$

In this formulation, homogeneous Neumann boundary condition for pressure is retained. An inhomogeneous boundary condition for u^* is introduced so that the slip velocity of u^{n+1} at the boundary is of order Δt^2.

[1] Here and in the following, the term "projection" should be understood in a more general sense than the Helmholtz decomposition since more general boundary conditions are allowed.

Remark. The nonlinear convection term $(\boldsymbol{u}^{n+1/2}\cdot\nabla)\boldsymbol{u}^{n+1/2}$ can be treated in many ways. In Theorems 3.2 and 3.4, we use an explicit Adams–Bashforth formula, $\frac{3}{2}(\boldsymbol{u}^n\cdot\nabla)\boldsymbol{u}^n - \frac{1}{2}(\boldsymbol{u}^{n-1}\cdot\nabla)\boldsymbol{u}^{n-1}$, which is the one used by Kim and Moin.

It is readily seen that the projection step enforces

$$\frac{\partial p^{n+1/2}}{\partial \boldsymbol{n}} = \frac{\partial p^{n-1/2}}{\partial \boldsymbol{n}} = \cdots = \frac{\partial p^{-1/2}}{\partial \boldsymbol{n}} \qquad \text{on } \partial\Omega \tag{2.13}$$

for the numerical solution. In general this is not satisfied by the exact solution of (2.1). Therefore we expect that $\frac{\partial p^{n+1/2}}{\partial \boldsymbol{n}}$ has $O(1)$ error at the boundary. As will be seen in §4, this causes $\boldsymbol{u}^*$ and $p^{n+1/2}$ to have numerical boundary layers.

(2) Projection method based on an accurate pressure boundary condition [19]:

$$\begin{cases} \dfrac{\boldsymbol{u}^* - \boldsymbol{u}^n}{\Delta t} + (\boldsymbol{u}^{n+1/2}\cdot\nabla)\boldsymbol{u}^{n+1/2} = \Delta\dfrac{\boldsymbol{u}^* + \boldsymbol{u}^n}{2}, \\ \boldsymbol{u}^* = 0 \qquad \text{on } \partial\Omega, \\ \boldsymbol{u}^* = \boldsymbol{u}^{n+1} + \Delta t \nabla p^{n+1/2}, \\ \nabla\cdot\boldsymbol{u}^{n+1} = 0, \\ \dfrac{\partial p^{n+1/2}}{\partial \boldsymbol{n}} = -\boldsymbol{n}\cdot[\nabla\times(\nabla\times\boldsymbol{u}^*)] \qquad \text{on } \partial\Omega. \end{cases} \tag{2.14}$$

In this formulation, the homogeneous Dirichlet boundary condition for the intermediate state $\boldsymbol{u}^*$ is retained. An inhomogeneous Neumann boundary condition for pressure is introduced so that the slip velocity of $\boldsymbol{u}^{n+1}$ at the boundary is of order $O(\Delta t^2)$.

The boundary condition for pressure in (2.14) is motivated by the first relation in (2.8). Notice that imposing (2.8) directly may not be consistent with the Poisson equation for pressure

$$\Delta p^{n+1/2} = \frac{1}{\Delta t}\nabla\cdot\boldsymbol{u}^*, \tag{2.15}$$

which implies

$$\int_{\partial\Omega} \frac{\partial p^{n+1/2}}{\partial \boldsymbol{n}}\, ds = 0. \tag{2.16}$$

However, the revised form of the pressure boundary condition is guaranteed to be consistent with the above relation. For more discussion see the end of §5.

(3) Projection method based on the pressure increment formulation [3], [4], [28]:

$$\begin{cases} \dfrac{\boldsymbol{u}^* - \boldsymbol{u}^n}{\Delta t} + (\boldsymbol{u}^{n+1/2}\cdot\nabla)\boldsymbol{u}^{n+1/2} + \nabla p^{n-1/2} = \Delta\dfrac{\boldsymbol{u}^* + \boldsymbol{u}^n}{2}, \\ \boldsymbol{u}^* = 0 \qquad \text{on } \partial\Omega, \\ \boldsymbol{u}^* = \boldsymbol{u}^{n+1} + \Delta t(\nabla p^{n+1/2} - \nabla p^{n-1/2}), \\ \nabla\cdot\boldsymbol{u}^{n+1} = 0, \\ \boldsymbol{n}\cdot\boldsymbol{u}^{n+1} = 0 \qquad \text{on } \partial\Omega. \end{cases} \tag{2.17}$$

Again the spurious slip velocity of $\boldsymbol{u}^{n+1}$ at the boundary is of order Δt^2, and the numerical solutions satisfy (2.13). If we let $\hat{\boldsymbol{u}} = \boldsymbol{u}^* - \Delta t \nabla p^{n-1/2}$ in (2.12), then we

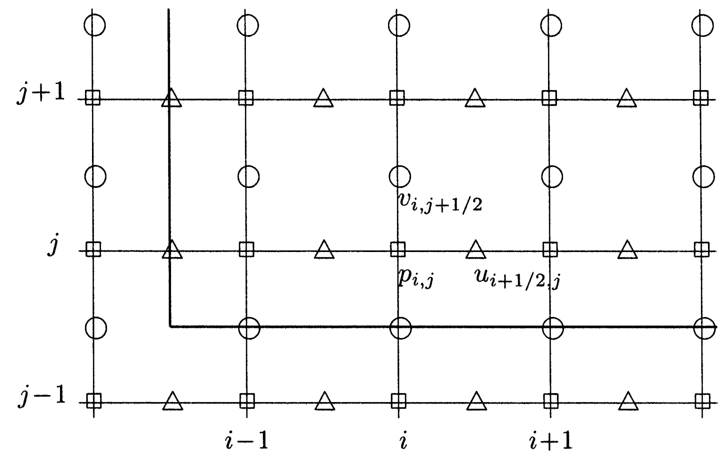

FIG. 1. *The MAC mesh.*

have

$$
(2.18)\quad \begin{cases} \dfrac{\hat{\boldsymbol{u}} - \boldsymbol{u}^n}{\Delta t} + (\boldsymbol{u}^{n+1/2} \cdot \nabla)\boldsymbol{u}^{n+1/2} + \nabla p^{n-1/2} = \Delta \dfrac{\hat{\boldsymbol{u}} + \boldsymbol{u}^n}{2} + \dfrac{\Delta t}{2} \Delta \nabla p^{n-1/2}, \\ \hat{\boldsymbol{u}} + u^n = 0 \qquad \text{on } \partial\Omega, \\ \hat{\boldsymbol{u}} = \boldsymbol{u}^{n+1} + \Delta t(\nabla p^{n+1/2} - \nabla p^{n-1/2}), \\ \nabla \cdot \boldsymbol{u}^{n+1} = 0, \\ \boldsymbol{n} \cdot \boldsymbol{u}^{n+1} = 0 \qquad \text{on } \partial\Omega. \end{cases}
$$

Except for the last term in the first equation, this is basically the same as (2.17). This suggests that (2.17) should behave similarly to (2.12). Surprisingly enough, (2.17) exhibits some peculiarities not shared by either (2.12) or (2.14). This will be the subject of a subsequent paper [9].

2.2. Spatial discretization. The remaining task is to solve the Poisson-type equations in (2.6)–(2.7), etc., instead of the coupled system of Stokes-like equations in (2.3) and (2.4). Any of the popular methods, such as finite difference, finite element, spectral, or spectral element, can be used for this purpose. In many cases, fast Poisson solvers or domain decomposition methods can be used to drastically speed up the calculation. When the Reynolds number is large, the NSE are effectively convection dominated. One can then borrow the techniques developed in the numerical solutions of hyperbolic equations or compressible flows. Such examples can be found in [3], [4], [20].

As an example of how the fully discrete schemes can be analyzed in the same fashion as the spatially continuous schemes, we consider in [10] the well-known spatial discretization scheme: centered difference on a staggered grid (also known as the MAC mesh), coupled with the time-splitting schemes.

An illustration of the MAC mesh near the boundary is given in Fig. 1, following the presentation of [1]. Here pressure is evaluated at the square points (i, j), the u velocity at the triangle points $(i \pm \frac{1}{2}, j)$, and the v velocity at the circle points $(i, j \pm \frac{1}{2})$.

The discrete divergence is computed at the square points:

$$(\nabla\cdot\boldsymbol{u})_{i,j} = \frac{u_{i+1/2,j} - u_{i-1/2,j}}{\triangle x} + \frac{v_{i,j+1/2} - v_{i,j-1/2}}{\triangle y}\,. \tag{2.19}$$

Other differential operators are discretized as

(2.20)

$$(\Delta u)_{i+1/2,j} = \frac{u_{i+3/2,j} - 2u_{i+1/2,j} + u_{i-1/2,j}}{\triangle x^2} + \frac{u_{i+1/2,j+1} - 2u_{i+1/2,j} + u_{i+1/2,j-1}}{\triangle y^2}\,,$$

$$(\Delta v)_{i,j+1/2} = \frac{v_{i+1,j+1/2} - 2u_{i,j+1/2} + u_{i-1,j+1/2}}{\triangle x^2} + \frac{v_{i,j+3/2} - 2v_{i,j+1/2} + v_{i,j-1/2}}{\triangle y^2}\,;$$

$$\begin{aligned} (p_x)_{i+1/2,j} &= \frac{p_{i+1,j} - p_{i,j}}{\triangle x}\,, \\ (p_y)_{i,j+1/2} &= \frac{p_{i,j+1} - p_{i,j}}{\triangle y}\,; \end{aligned} \tag{2.21}$$

$$\begin{aligned} \bar{u}_{i,j+1/2} &= \tfrac{1}{4}\big(u_{i+1/2,j} + u_{i-1/2,j} + u_{i+1/2,j+1} + u_{i-1/2,j+1}\big)\,, \\ \bar{v}_{i+1/2,j} &= \tfrac{1}{4}\big(v_{i+1,j+1/2} + v_{i+1,j-1/2} + v_{i,j+1/2} + v_{i,j-1/2}\big)\,; \end{aligned} \tag{2.22}$$

(2.23)

$$(\boldsymbol{u}\cdot\nabla a)_{i+1/2,j} = u_{i+1/2,j}\frac{a_{i+3/2,j} - a_{i-1/2,j}}{2\triangle x} + \bar{v}_{i+1/2,j}\frac{a_{i+1/2,j+1} - a_{i+1/2,j-1}}{2\triangle y}\,,$$

$$(\boldsymbol{u}\cdot\nabla b)_{i,j+1/2} = \bar{u}_{i,j+1/2}\frac{b_{i+1,j+1/2} - b_{i-1,j+1/2}}{2\triangle x} + v_{i,j+1/2}\frac{b_{i,j+3/2} - b_{i,j-1/2}}{2\triangle y}\,;$$

$$\mathcal{N}_h(\boldsymbol{u},\boldsymbol{a}) = \big((\boldsymbol{u}\cdot\nabla a)_{i+1/2,j}, (\boldsymbol{u}\cdot\nabla b)_{i,j+1/2}\big)\,. \tag{2.24}$$

The boundary condition $u = 0$ is imposed at the vertical physical boundary, whereas $v = 0$ is imposed at the "ghost" circle points which are $\triangle x/2$ to the left or right of the physical boundary. Similarly the boundary condition $v = 0$ is imposed at the horizontal physical boundary, but $u = 0$ is imposed at the "ghost" triangle points with a distance of $\triangle y/2$ away from the physical boundary.

Notations. We will use C to denote generic constants which may depend on the norms of the exact solutions. Norms will be taken over the entire domain Ω.

3. Summary of results and outline of proofs. For simplicity of presentation, we will concentrate on the situation when $\Omega = [-1,1]\times[0,2\pi]$ with periodic boundary condition in the y-direction and no-slip boundary condition in the x-direction: $\boldsymbol{u}(x,0,t) = \boldsymbol{u}(x,2\pi,t), \boldsymbol{u}(-1,y,t) = 0, \boldsymbol{u}(1,y,t) = 0$. We will use $\partial'\Omega$ to denote the part of the boundary at $x = \pm 1$ where the no-slip boundary condition is applied. We will always assume that $\triangle x \sim \triangle y$ and $h = \min(\triangle x, \triangle y)$. Extensions to general domains will be discussed in §7. We will concentrate our discussions on the spatially continuous schemes since the main issue is in the temporal-discretization, as we have illustrated above.

The main results of this paper are the following (the constants are independent of $\triangle t$ and h).

THEOREM 3.1. *Let $(\boldsymbol{u}, p)$ be a smooth solution of the Navier–Stokes equation* (2.1) *with smooth initial data $\boldsymbol{u}^0(\boldsymbol{x})$ and let $(\boldsymbol{u}_{\triangle t}, p_{\triangle t})$ be the numerical solution for the semidiscrete projection method* (2.6), (2.7), *and* (2.10). *Then we have*

$$\|\boldsymbol{u} - \boldsymbol{u}_{\triangle t}\|_{L^\infty(0,T;L^2)} + \triangle t^{1/2}\, \|p - p_{\triangle t}\|_{L^2(0,T;L^2)} \le C\triangle t. \tag{3.1}$$

Furthermore, if $\boldsymbol{u}^0(\boldsymbol{x})$ satisfies the compatibility condition

$$\boldsymbol{u}^0(\boldsymbol{x}) = 0\,, \quad \partial_y p(\boldsymbol{x}, 0) = \partial^2_{xy} p(\boldsymbol{x}, 0) = 0 \quad \text{on } \partial^{'}\Omega, \tag{3.2}$$

then we have

$$\|\boldsymbol{u} - \boldsymbol{u}_{\triangle t}\|_{L^\infty} + \triangle t^{1/2} \|p - p_{\triangle t}\|_{L^\infty} \le C\triangle t\,, \tag{3.3}$$

$$\|p - p_{\triangle t} - p_c\|_{L^\infty} \le C\triangle t, \tag{3.4}$$

where

$$\begin{aligned} p_c(\boldsymbol{x}, t) \quad &\equiv \triangle t^{1/2} \frac{e}{e-1} e^{-|x-1|/\triangle t^{1/2}}\, \partial_x p_{\triangle t}(x - \triangle t^{1/2}, y, t) \\ &+ \triangle t^{1/2} \frac{e}{e-1} e^{-|x+1|/\triangle t^{1/2}}\, \partial_x p_{\triangle t}(x + \triangle t^{1/2}, y, t)\,. \end{aligned}$$

Remark. It is rather common to require compatibility conditions on the initial data in order to get full accuracy of a numerical scheme, although here we require more than necessary. We refer to the work of Heywood and Rannacher [14] and Okamoto [18] on discussions of minimum compatibility assumptions.

THEOREM 3.2. *Let $(\boldsymbol{u}, p)$ be a smooth solution of the Navier–Stokes equation* (2.1) *with smooth initial data $\boldsymbol{u}^0(\boldsymbol{x})$ and let $(\boldsymbol{u}_{\triangle t}, p_{\triangle t})$ be the numerical solution for the semidiscrete projection method* (2.12). *Then we have*

$$\|\boldsymbol{u} - \boldsymbol{u}_{\triangle t}\|_{L^\infty(0,T;L^2)} + \triangle t \|p - p_{\triangle t}\|_{L^\infty(0,T;L^2)} \le C\triangle t^2. \tag{3.5}$$

Furthermore, if $\boldsymbol{u}^0(\boldsymbol{x})$ satisfies the compatibility condition

$$\partial_x^{\alpha_1} \partial_y^{\alpha_2} \boldsymbol{u}^0(\boldsymbol{x}) = 0 \quad \text{on } \partial^{'}\Omega \quad \text{for } \alpha_1 + \alpha_2 \le 6\,, \tag{3.6}$$

then we have

$$\|\boldsymbol{u} - \boldsymbol{u}_{\triangle t}\|_{L^\infty} + \triangle t^{3/2} \|p - p_{\triangle t}\|_{L^\infty} \le C\triangle t^2\,, \tag{3.7}$$

$$\max_{\mathrm{dist}(\boldsymbol{x} - \partial'\Omega) \ge \triangle t^{1/2}} |p - p_{\triangle t}| \le C\triangle t^2\,, \tag{3.8}$$

$$\|p - p_{\triangle t} - p_c\|_{L^\infty} \le C\triangle t\,, \tag{3.9}$$

where

$$\begin{aligned} p_c(\boldsymbol{x},t) \quad &\equiv \sqrt{\frac{\Delta t}{2}}\frac{e^{\sqrt{2}}}{e^{\sqrt{2}}-1}e^{-\sqrt{2}|x-1|/\Delta t^{1/2}}\partial_x p_{\Delta t}(x-\Delta t^{1/2},y,t) \\ &+\sqrt{\frac{\Delta t}{2}}\frac{e^{\sqrt{2}}}{e^{\sqrt{2}}-1}e^{-\sqrt{2}|x+1|/\Delta t^{1/2}}\partial_x p_{\Delta t}(x+\Delta t^{1/2},y,t). \end{aligned}$$

Remark. The Appendix contains a discussion on how to remove the next order boundary layer errors in the numerical approximations of pressure to get a uniform $O(\Delta t^2)$ convergence rate.

THEOREM 3.3. *Let $(\boldsymbol{u},p)$ be a solution of the Navier–Stokes equation* (2.1) *with smooth initial data $\boldsymbol{u}^0(\boldsymbol{x})$ satisfying the compatibility condition*

$$\boldsymbol{u}^0(\boldsymbol{x})=0\,,\quad \partial_y p(\boldsymbol{x},0)=\partial^2_{xy}p(\boldsymbol{x},0)=0\quad \text{on } \partial^{'}\Omega. \tag{3.10}$$

Let $(\boldsymbol{u}_h,p_h)$ be the numerical solution of the projection method (2.6), (2.7), *and* (2.10) *coupled with the MAC spatial discretization. Assume that $\Delta t << h$. Then we have*

$$\|\boldsymbol{u}-\boldsymbol{u}_h\|_{L^\infty}+\Delta t^{1/2}\|p-p_h\|_{L^\infty}\le C(\Delta t+h^2)\,, \tag{3.11}$$

$$\|p-p_h-p_c\|_{L^\infty}\le C(\Delta t+h^2)\,, \tag{3.12}$$

where

$$\begin{aligned} p_c(\boldsymbol{x},t) \quad &\equiv \Delta t^{1/2}\beta\frac{e^{\alpha}}{e^{\alpha}-1}\,e^{-\alpha|x-1|/\Delta t^{1/2}}\,D^x_+p_h(x-\Delta t^{1/2},y,t) \\ &+\Delta t^{1/2}\beta\frac{e^{\alpha}}{e^{\alpha}-1}\,e^{-\alpha|x+1|/\Delta t^{1/2}}\,D^x_+p_h(x+\Delta t^{1/2},y,t), \end{aligned} \tag{3.13}$$

$$\alpha=\frac{\Delta t^{1/2}}{\Delta x}\text{arccosh}\left(1+\frac{\Delta x^2}{2\Delta t}\right),\qquad \beta=\frac{\Delta x}{\Delta t^{1/2}}(1-e^{-\alpha\Delta x/\Delta t^{1/2}})^{-1}.$$

THEOREM 3.4. *Let $(\boldsymbol{u},p)$ be a smooth solution of the Navier–Stokes equation* (2.1) *with smooth initial data $\boldsymbol{u}^0(\boldsymbol{x})$ satisfying the compatibility condition*

$$\partial_x^{\alpha_1}\partial_y^{\alpha_2}\boldsymbol{u}^0(\boldsymbol{x})=0\quad \text{on } \partial\Omega\quad \text{for } \alpha_1+\alpha_2\le 6. \tag{3.14}$$

Let $(\boldsymbol{u}_h,p_h)$ be the numerical solution of the projection method (2.12) *coupled with the MAC spatial discretization. Assume that $\Delta t^2 << h$. Then we have*

$$\|\boldsymbol{u}-\boldsymbol{u}_h\|_{L^\infty}+\Delta t^{3/2}\|p-p_h\|_{L^\infty}+\Delta t\|p-p_h\|_{L^\infty(0,T;L^2)}\le C(\Delta t^2+h^2), \tag{3.15}$$

$$\|p-p_h-p_c\|_{L^\infty}\le C(\Delta t+h^2)\,, \tag{3.16}$$

where

$$\begin{aligned} p_c \quad &\equiv \Delta t^{1/2}\beta\frac{e^{\alpha}}{e^{\alpha}-1}\,e^{-\alpha|x-1|/\Delta t^{1/2}}\,D^x_+p_h(x-\Delta t^{1/2},y,t) \\ &+\Delta t^{1/2}\beta\frac{e^{\alpha}}{e^{\alpha}-1}\,e^{-\alpha|x+1|/\Delta t^{1/2}}\,D^x_+p_h(x+\Delta t^{1/2},y,t), \end{aligned} \tag{3.17}$$

$$\alpha = \frac{\Delta t^{1/2}}{\Delta x}\operatorname{arccosh}\left(1 + \frac{\Delta x^2}{\Delta t}\right), \qquad \beta = \frac{\Delta x}{\Delta t^{1/2}}(1 - e^{-\alpha \Delta x/\Delta t^{1/2}})^{-1}.$$

Remark. We refer to §7 for extensions to general domains.

There are three major steps in the proofs of these results. Here we illustrate these steps for the first-order scheme (2.6), (2.7), and (2.10).

Step 1. Using boundary layer analysis, we construct approximate solutions of the form ($t^n = n\Delta t$):

$$\begin{aligned} U^*(\boldsymbol{x}, t^n) &= \boldsymbol{u}_0^*(\boldsymbol{x}, t^n) + \Delta t^{1/2}\ \boldsymbol{u}_1^*(\boldsymbol{x}, (x \pm 1)/\Delta t^{1/2}, t^n) + \cdots, \\ U^n(\boldsymbol{x}, t^n) &= \boldsymbol{u}_0(\boldsymbol{x}, t^n) + \Delta t^{1/2}\ \boldsymbol{u}_1(\boldsymbol{x}, (x \pm 1)/\Delta t^{1/2}, t^n) + \cdots, \\ P^n(\boldsymbol{x}, t^n) &= p_0(\boldsymbol{x}, t^n) + \Delta t^{1/2}\ p_1(\boldsymbol{x}, (x \pm 1)/\Delta t^{1/2}, t^n) + \cdots, \end{aligned} \tag{3.18}$$

satisfying the numerical scheme to high-order accuracy:

$$\begin{cases} \dfrac{U^* - U^n}{\Delta t} + (U^n \cdot \nabla) U^n = \Delta U^* + \Delta t^\alpha \boldsymbol{f}^n, \\ U^* = 0 \qquad \text{on } \partial\Omega, \\ \dfrac{U^{n+1} - U^*}{\Delta t} + \nabla P^n = \Delta t^\alpha \boldsymbol{g}^n, \\ \nabla \cdot U^{n+1} = 0, \\ U^{n+1} \cdot \boldsymbol{n} = 0 \qquad \text{on } \partial\Omega, \\ U^0 = \boldsymbol{u}^0 + \Delta t^\alpha \boldsymbol{w}^0, \end{cases} \tag{3.19}$$

where α is a predetermined number.

Step 2. The L^2-stability of these numerical schemes can be proved using energy estimates. Together with (2.6), (2.7), (2.10), and (3.19), we get

$$\begin{aligned} \|\boldsymbol{u}^n - U^n\|_{L^2} &\le C^*\ \Delta t^\alpha, \\ \|\boldsymbol{u}^* - U^*\|_{L^2} &\le C^*\ \Delta t^\alpha, \\ \|p^n - P^n\|_{L^2} &\le C^*\ \Delta t^{\alpha - 1}, \end{aligned} \tag{3.20}$$

where the constant C^* depends on

$$|||\boldsymbol{u}^n|||_{L^\infty} = \sup_{0 \le t \le T} \|\boldsymbol{u}^n(\cdot, t)\|_{L^\infty}.$$

Step 3. To complete the proof, we need to

(1) establish a priori estimates on $|||\boldsymbol{u}^n|||_{L^\infty}$;

(2) convert the L^2 estimates in (3.20) to L^∞ estimates.

The standard way of achieving (1) and (2) for fully discrete methods is to use the inverse inequality:

$$\|\boldsymbol{u}_h\|_{L^\infty} \le h^{-d/2} \|\boldsymbol{u}_h\|_{L^2},$$

where h is the spatial mesh size, and d is the dimension. This is also the major component of Strang and Michelson's analysis. This standard trick is used to prove

Theorems 3.3 and 3.4 for the fully discrete schemes. However, this trick cannot be used to prove Theorems 3.1 and 3.2, which deal with the spatially continuous schemes. In this case, we get (1) and (2) directly by using careful a priori estimates and the regularity theory for elliptic equations.

The actual proofs are quite complicated. In the next section, we provide the detailed proof of Theorem 3.1. The proof of Theorem 3.2 is analogous although some details in estimates are different. This is done in §6. The proof of Theorems 3.3 and 3.4 for the fully discrete schemes goes along the same line. The details of that can be found in [10].

4. First-order schemes without spatial discretization. We will concentrate on the following version of the first-order projection method:

$$\begin{cases} \dfrac{\boldsymbol{u}^* - \boldsymbol{u}^n}{\Delta t} + (\boldsymbol{u}^n \cdot \nabla)\boldsymbol{u}^n = \Delta \boldsymbol{u}^* \,, \\ \boldsymbol{u}^* = 0 \qquad \text{on } \partial\Omega \,, \\ \boldsymbol{u}^* = \boldsymbol{u}^{n+1} + \Delta t \nabla p^n \,, \\ \nabla \cdot \boldsymbol{u}^{n+1} = 0 \,, \\ \dfrac{\partial p^n}{\partial \boldsymbol{n}} = 0 \qquad \text{on } \partial\Omega \,. \end{cases} \tag{4.1}$$

The corresponding fully discrete scheme with the standard MAC spatial discretization is studied in [10]. Many variants of (4.1) are possible. Some of them are discussed in the next section.

4.1. Asymptotic analysis of the numerical solutions. Denote the solutions of (4.1) as $(\boldsymbol{u}_{\Delta t}, \boldsymbol{u}^*_{\Delta t}, p_{\Delta t})$. Motivated by the discussions in §2, we make the following ansatz, valid at $t^n = n\Delta t$, $n = 1, 2, \ldots$,

$$\begin{cases} \boldsymbol{u}^*_{\Delta t}(\boldsymbol{x}, t) = \boldsymbol{u}^*_0(\boldsymbol{x}, t) + \displaystyle\sum_{j=1} \varepsilon^j [\boldsymbol{u}^*_j(\boldsymbol{x}, t) + \boldsymbol{a}^*_j(\xi, y, t)] \,, \\ \boldsymbol{u}_{\Delta t}(\boldsymbol{x}, t) = \boldsymbol{u}_0(\boldsymbol{x}, t) + \displaystyle\sum_{j=1} \varepsilon^j \boldsymbol{u}_j(\boldsymbol{x}, t) \,, \\ p_{\Delta t}(\boldsymbol{x}, t) = p_0(\boldsymbol{x}, t) + \varphi_0(\xi, y, t) + \displaystyle\sum_{j=1} \varepsilon^j [p_j(\boldsymbol{x}, t) + \varphi_j(\xi, y, t)] \,. \end{cases} \tag{4.2}$$

Here $\varepsilon = \Delta t^{1/2}$, $\xi = (x+1)/\varepsilon, \boldsymbol{u}^*_j = (u^*_j, v^*_j), \boldsymbol{a}^*_j = (a^*_j, b^*_j), \boldsymbol{u}_j = (u_j, v_j)$. We assume that the ξ-dependent functions decay super algebraically as $\xi \to +\infty$. In doing so, we have committed our attention to the left boundary at $x = -1$. Clearly a similar analysis can be done at the right boundary $\{x = 1\}$. Our purpose is to find the coefficients in this expansion such that the truncated series satisfies (4.1) to high-order accuracy. Using the notation $\nabla_\xi = (\partial_\xi, 0)$, $\nabla_y = (0, \partial_y)$, we have

$$\Delta \boldsymbol{u}^*_{\Delta t} = \Delta_{\boldsymbol{x}} \boldsymbol{u}^*_0 + \sum_{j=1} \varepsilon^j (\Delta_{\boldsymbol{x}} \boldsymbol{u}^*_j + \varepsilon^{-2} \partial^2_\xi \boldsymbol{a}^*_j + \partial^2_y \boldsymbol{a}^*_j) \,, \tag{4.3}$$

$$\nabla \cdot \boldsymbol{u}_{\Delta t} = \nabla_{\boldsymbol{x}} \cdot \boldsymbol{u}_0 + \sum_{j=1} \varepsilon^j \nabla_{\boldsymbol{x}} \cdot \boldsymbol{u}_j \,, \tag{4.4}$$

$$\nabla p_{\triangle t} = \nabla_{\boldsymbol{x}} p_0 + \varepsilon^{-1}\nabla_\xi \varphi_0 + \nabla_y \varphi_0 + \sum_{j=1} \varepsilon^j (\nabla_{\boldsymbol{x}} p_j + \varepsilon^{-1}\nabla_\xi \varphi_j + \nabla_y \varphi_j), \tag{4.5}$$

$$\begin{aligned} \boldsymbol{u}^{n+1}(\boldsymbol{x}) &= \boldsymbol{u}_0(\boldsymbol{x}, t^{n+1}) + \sum_{j=1} \varepsilon^j \boldsymbol{u}_j(\boldsymbol{x}, t^{n+1}) \\ &= \sum_{k=0} \frac{1}{k!}\varepsilon^{2k}\boldsymbol{u}_0^{(k)}(\boldsymbol{x}, t^n) + \sum_{j=1}\varepsilon^j \sum_{k=0}\frac{1}{k!}\varepsilon^{2k}\boldsymbol{u}_j^{(k)}(\boldsymbol{x}, t^n). \end{aligned} \tag{4.6}$$

From now on we will omit the subscript $\boldsymbol{x}$ for operators with respect to $\boldsymbol{x}$.

Next we substitute these relations into (4.1) in order to determine the coefficients of ε^j in (4.2). We get hierarchies of equations by collecting equal powers of ε.

The first equation in (4.1) gives

$$\boldsymbol{u}_0^* = \boldsymbol{u}_0, \tag{4.7}$$

$$\boldsymbol{u}_1^* + \boldsymbol{a}_1^* - \boldsymbol{u}_1 = \partial_\xi^2 \boldsymbol{a}_1^*, \tag{4.8}$$

$$\boldsymbol{u}_2^* + \boldsymbol{a}_2^* - \boldsymbol{u}_2 + (\boldsymbol{u}_0\cdot\nabla)\boldsymbol{u}_0 = \Delta^2 \boldsymbol{u}_0^* + \Delta_\xi^2 \boldsymbol{a}_2^*. \tag{4.9}$$

For $j \geq 1$,

$$\boldsymbol{u}_{j+2}^* + \boldsymbol{a}_{j+2}^* - \boldsymbol{u}_{j+2} + \sum_{k=0}^{j} (\boldsymbol{u}_k\cdot\nabla)\boldsymbol{u}_{j-k} = \Delta \boldsymbol{u}_j^* + \partial_\xi^2 \boldsymbol{a}_{j+2}^* + \partial_y^2 \boldsymbol{a}_j^*. \tag{4.10}$$

The second equation in (4.1) implies

$$\boldsymbol{u}_0^* = \boldsymbol{u}_0, \tag{4.11}$$

$$\boldsymbol{u}_1^* + \boldsymbol{a}_1^* = \boldsymbol{u}_1 + \nabla_\xi \varphi_0, \tag{4.12}$$

$$\boldsymbol{u}_2^* + \boldsymbol{a}_2^* = \boldsymbol{u}_2 + \partial_t \boldsymbol{u}_0 + \nabla p_0 + \nabla_\xi \varphi_1 + \nabla_y \varphi_0. \tag{4.13}$$

For $j = 2\ell - 1$, $\ell \geq 1$,

$$\boldsymbol{u}_{j+2}^* + \boldsymbol{a}_{j+2}^* = \boldsymbol{u}_{j+2} + \partial_t \boldsymbol{u}_j + \nabla p_j + \nabla_\xi \varphi_{j+1} + \nabla_y \varphi_j + \sum_{k=2}^{\ell} \frac{1}{k!}\boldsymbol{u}_{j-2k+2}^{(k)}. \tag{4.14}$$

For $j = 2\ell$, $\ell \geq 1$,

$$\begin{aligned} \boldsymbol{u}_{j+2}^* + \boldsymbol{a}_{j+2}^* &= \boldsymbol{u}_{j+2} + \partial_t \boldsymbol{u}_j + \nabla p_j + \nabla_\xi \varphi_{j+1} + \nabla_y \varphi_j \\ &\quad + \frac{1}{(\ell+1)!}\boldsymbol{u}_0^{(\ell+1)} + \sum_{k=2}^{\ell} \frac{1}{k!}\boldsymbol{u}_{j-2k+2}^{(k)}. \end{aligned} \tag{4.15}$$

From the third equation in (4.1), we obtain

$$\nabla\cdot \boldsymbol{u}_j = 0, \qquad j = 0, 1, \dots. \tag{4.16}$$

The boundary conditions become

$$\boldsymbol{u}_0^* = 0, \quad \partial_\xi \varphi_0 = 0, \quad \text{at} \quad x = -1, \quad \xi = 0\,, \tag{4.17}$$

$$\boldsymbol{u}_j^* + \boldsymbol{a}_j^* = 0\,, \quad \partial_x p_{j-1} + \partial_\xi \varphi_j = 0\,, \quad \text{at} \quad x = -1, \quad \xi = 0 \tag{4.18}$$

for $j > 0$.

Our next task is to analyze these equations to see whether they are solvable. We begin by noticing that (4.8) and (4.12) imply

$$\boldsymbol{u}_1^* = \boldsymbol{u}_1\,, \tag{4.19}$$

$$\boldsymbol{a}_1^* = \partial_\xi^2 \boldsymbol{a}_1^* = \nabla_\xi \varphi_0 \tag{4.20}$$

since $\boldsymbol{u}_1^*$ and $\boldsymbol{u}_1$ do not depend on ξ. From (4.17), we get

$$\boldsymbol{a}_1^* = 0\,, \quad \varphi_0 = 0\,. \tag{4.21}$$

Next we collect the ξ-independent part of (4.9), (4.13), and (4.16) to obtain

$$\begin{cases} \partial_t \boldsymbol{u}_0 + \nabla p_0 + (\boldsymbol{u}_0 \cdot \nabla)\boldsymbol{u}_0 = \Delta \boldsymbol{u}_0\,, \\ \nabla \cdot \boldsymbol{u}_0 = 0. \end{cases} \tag{4.22}$$

The remaining part of the these equations gives

$$\boldsymbol{a}_2^* = \partial_\xi^2 \boldsymbol{a}_2^*\,, \tag{4.23}$$

$$\boldsymbol{a}_2^* = \nabla_\xi \varphi_1 + \nabla_y \varphi_0\,. \tag{4.24}$$

Not surprisingly, the leading-order terms in (4.2) satisfy the original NSE (4.22) with the boundary condition $\boldsymbol{u}_0 = 0$ on $\partial' \Omega$. It is natural to associate (4.22) with the initial condition $\boldsymbol{u}_0(\boldsymbol{x}, 0) = \boldsymbol{u}^0(\boldsymbol{x})$. It is easy to see that (4.23)–(4.24) are satisfied if we choose

$$b_2^* = 0\,, \quad a_2^* = \partial_\xi \varphi_1\,, \tag{4.25}$$

$$\varphi_1 = \partial_\xi^2 \varphi_1\,. \tag{4.26}$$

The boundary condition for (4.26) can be obtained from (4.18) with $j = 1$:

$$\partial_\xi \varphi_1 + \partial_x p_0 = 0\,, \quad \text{at} \quad \xi = 0, \quad x = -1\,. \tag{4.27}$$

(4.26) and (4.27) imply

$$\varphi_1(\xi, y, t) = \partial_x p_0(-1, y, t)\, e^{-\xi}\,. \tag{4.28}$$

So far we have obtained solutions for $\boldsymbol{u}_0^*, \boldsymbol{u}_0, p_0, \boldsymbol{a}_1^*, \varphi_0, \boldsymbol{a}_2^*, \varphi_1$. Let $j = 1$ in (4.10), $j = 3$ in (4.14), and $j = 1$ in (4.16); we get

$$\begin{cases} \partial_t \boldsymbol{u}_1 + \nabla p_1 + (\boldsymbol{u}_0 \cdot \nabla)\boldsymbol{u}_1 + (\boldsymbol{u}_1 \cdot \nabla)\boldsymbol{u}_0 = \Delta \boldsymbol{u}_1\,, \\ \nabla \cdot \boldsymbol{u}_1 = 0\,, \end{cases} \tag{4.29}$$

$$\left\{\begin{array}{l} \boldsymbol{a}_3^* = \partial_\xi^2 \boldsymbol{a}_3^* \,, \\ \boldsymbol{a}_3^* = \nabla_\xi \varphi_2 + \nabla_y \varphi_1 \,. \end{array}\right. \tag{4.30}$$

The boundary condition for (4.29) is $\boldsymbol{u}_1|_{\partial' \Omega} = 0$. The initial data for (4.29) is $\boldsymbol{u}_1 \,|_{t=0} = 0$. Therefore we have

$$\boldsymbol{u}_1 = 0 \,, \quad p_1 = 0 \,. \tag{4.31}$$

From (4.18) and (4.30), we have

$$\partial_\xi \varphi_2 = 0 \,, \quad \text{at} \quad x = -1, \quad \xi = 0 \,. \tag{4.32}$$

The solutions of (4.30) and (4.32) are given by

$$\varphi_2 = 0 \,, \quad b_3^* = \partial_y \varphi_1, \quad a_3^* = 0 \,. \tag{4.33}$$

These give us $(\boldsymbol{u}_1^*, \boldsymbol{u}_1, p_1, \boldsymbol{a}_3^*, \varphi_2)$. Similarly, we have the next set of equations:

$$\left\{\begin{array}{l} \partial_t \boldsymbol{u}_2 + \nabla p_2 + (\boldsymbol{u}_0 \cdot \nabla) \boldsymbol{u}_2 + (\boldsymbol{u}_2 \cdot \nabla) \boldsymbol{u}_0 \\ \qquad = \Delta \boldsymbol{u}_2 + \Delta(\partial_t \boldsymbol{u}_0 + \nabla p_0) - \frac{1}{2} \partial_t^2 \boldsymbol{u}_0 \,, \\ \nabla \cdot \boldsymbol{u}_2 = 0 \,, \end{array}\right. \tag{4.34}$$

$$\left\{\begin{array}{l} \boldsymbol{a}_4^* = \partial_\xi^2 \boldsymbol{a}_4^* + \partial_y^2 \boldsymbol{a}_2^* \,, \\ \boldsymbol{a}_4^* = \nabla_\xi \varphi_3 + \nabla_y \varphi_2 \,. \end{array}\right. \tag{4.35}$$

The boundary conditions can be obtained from (4.18) and (4.13):

$$\boldsymbol{u}_2 + \nabla p_0 + \nabla_\xi \varphi_1 = 0 \,, \quad \text{at} \quad \xi = 0, \quad x = -1, \tag{4.36}$$

$$\partial_\xi \varphi_3 + \partial_x p_2 = 0 \,, \quad \text{at} \quad \xi = 0, \quad x = -1 \,. \tag{4.37}$$

However, choosing the right initial data for (4.34) is a rather subtle issue. We will defer the discussion to the end of this subsection.

Notice that (4.36) and (4.27) imply that $\boldsymbol{u}_2 \cdot \boldsymbol{n} = 0$ on $\partial' \Omega$. In general, (4.14), (4.15), and (4.18) imply that this is true for all $\boldsymbol{u}_j$.

Solutions of (4.35), (4.37) are given by

$$b_4^* = 0 \,, \quad a_4^* = \partial_\xi \varphi_3 \,. \tag{4.38}$$

$$\varphi_3(\xi, y, t) = (\partial_x p_2 + \tfrac{1}{2} \partial_x \partial_y^2 p_0) \,|_{x=-1}\, e^{-\xi} + \tfrac{1}{2} \partial_x \partial_y^2 p_0 \,|_{x=-1}\, \xi e^{-\xi} \,. \tag{4.39}$$

This set of equations determines $(\boldsymbol{u}_2^*, \boldsymbol{u}_2, p_2, \boldsymbol{a}_4^*, \varphi_3)$. If we now look at the next equation in each of the groups (4.10), (4.14), and (4.16), we obtain

$$\left\{\begin{array}{l} \partial_t \boldsymbol{u}_3 + \nabla p_3 + (\boldsymbol{u}_0 \cdot \nabla) \boldsymbol{u}_3 + (\boldsymbol{u}_3 \cdot \nabla) \boldsymbol{u}_0 = \Delta \boldsymbol{u}_3 + \Delta \nabla p_2 \,, \\ \nabla \cdot \boldsymbol{u}_3 = 0 \,, \end{array}\right. \tag{4.40}$$

$$\boldsymbol{a}_5^* = \partial_\xi^2 \boldsymbol{a}_5^* + \partial_y^2 \boldsymbol{a}_3^* \,, \tag{4.41}$$

(4.42) $$a_5^* = \partial_\xi \varphi_4, \quad b_5^* = \partial_y \varphi_3 .$$

Usually one would expect that $(\boldsymbol{u}_3, p_3) = 0$, since they are the coefficients of $\triangle t^{3/2}$ terms. But the boundary layer in p gives rise to a nonzero boundary condition for (4.40). This is seen from (4.14), which for $j = 3$ reads

(4.43) $$\boldsymbol{u}_3^* + \boldsymbol{a}_3^* = \boldsymbol{u}_3 + \partial_t \boldsymbol{u}_1 + \nabla p_1 + \nabla_\xi \varphi_2 + \nabla_y \varphi_1 = \boldsymbol{u}_3 + \nabla_y \varphi_1 .$$

Therefore (4.18) implies that

(4.44) $$\boldsymbol{u}_3 + \nabla_y \varphi_1 = 0 , \quad \text{at} \quad x = -1, \quad \xi = 0 .$$

(4.40) and (4.44), together with a suitable initial condition that matches (4.44) at $t = 0$, determine $(\boldsymbol{u}_3, p_3)$. This in turn determines the boundary condition for φ_4,

(4.45) $$\partial_\xi \varphi_4 = -\partial_x p_3, \quad \text{at} \quad \xi = 0, \quad x = -1 .$$

(4.41) and (4.45) can be solved for φ_4, etc. This set of equations determines $(\boldsymbol{u}_3^*, \boldsymbol{u}_3,$ p_3, $\boldsymbol{a}_5^*, \varphi_4)$. Obviously this procedure can be continued and we obtain

(4.46) $$a_j^* = \partial_\xi \varphi_{j-1} , \quad b_j^* = \partial_y \varphi_{j-2} ,$$

(4.47) $$\varphi_j = \partial_\xi^2 \varphi_j + \partial_y^2 \varphi_{j-2},$$

(4.48) $$\varphi_j = \sum_{k=0}^{[j/2]} F_{j,k}(y) \xi^k e^{-\xi}.$$

Now if we let

(4.49) $$\begin{cases} U^* = \boldsymbol{u}_0^* + \displaystyle\sum_{j=1}^{2N} \varepsilon^j (\boldsymbol{u}_j^* + \boldsymbol{a}_j^*) , \\ U^n = \boldsymbol{u}_0 + \displaystyle\sum_{j=1}^{2N} \varepsilon^j \boldsymbol{u}_j , \\ P^n = p_0 + \displaystyle\sum_{j=1}^{2N} \varepsilon^j (p_j + \varphi_j) + \varepsilon^{2N+1} \varphi_{2N+1} , \end{cases}$$

then we have

(4.50) $$\begin{cases} \dfrac{U^* - U^n}{\triangle t} + (U^n \cdot \nabla) U^n = \Delta U^* + \triangle t^{N-1/2} \boldsymbol{f}_N , \\ U^* = 0 \qquad \text{on } \partial' \Omega , \\ U^* = U^{n+1} + \triangle t \nabla P^n + \triangle t^{N+1/2} \boldsymbol{g}_N , \\ \nabla \cdot U^{n+1} = 0 , \\ \dfrac{\partial P^n}{\partial \boldsymbol{n}} = \boldsymbol{n} \cdot U^{n+1} = 0 \qquad \text{on } \partial' \Omega , \end{cases}$$

where the coefficients $\boldsymbol{f}_N$ and $\boldsymbol{g}_N$ are functionals of $(\boldsymbol{u}_0, p_0)$. They are bounded and smooth if $(\boldsymbol{u}_0, p_0)$ are sufficiently smooth.

We now come to the choice of initial conditions. If we do not require extra compatibility conditions for the initial data $\boldsymbol{u}^0(\boldsymbol{x})$, then to have solutions $(\boldsymbol{u}_2, p_2)$ that are smooth at $t = 0$, we need to choose an initial data for $\boldsymbol{u}_2$ that matches (4.36). While there is no difficulty in doing this, it restricts the approximation of the initial data to

$$U^0(\boldsymbol{x}) = \boldsymbol{u}_0(\boldsymbol{x}, 0) + \triangle t \boldsymbol{w}^0(\boldsymbol{x}) \tag{4.51}$$

where $\boldsymbol{w}^0$ is a bounded function. This is enough for proving the L^2 estimate, but not enough for proving the L^∞ estimate.

However, if we assume that the initial data $\boldsymbol{u}^0(\boldsymbol{x})$ for NSE (2.1) satisfies the following compatibility condition

$$\boldsymbol{u}^0(\boldsymbol{x}) = 0\,, \quad \partial_y p_0 = 0 \quad \text{on } \partial' \Omega\,, \tag{4.52}$$

then we can choose

$$\boldsymbol{u}_2(\boldsymbol{x}, 0) = 0 \tag{4.53}$$

since

$$\boldsymbol{u}_2 \,|_{x=-1,t=0} = -\nabla p_0 \,|_{x=-1,t=0} - \nabla_\xi \varphi_1 \,|_{\xi=0,t=0} = (0, -\partial_y p_0 \,|_{x=-1,t=0}) = 0\,. \tag{4.54}$$

Likewise, if we assume

$$\partial_x \partial_y p_0 = 0 \qquad \text{on } \partial' \Omega, \tag{4.55}$$

then we have

$$\boldsymbol{u}_3(\boldsymbol{x}, 0) = 0\,. \tag{4.56}$$

Hence we have

$$U^0(\boldsymbol{x}) = \boldsymbol{u}_0(\boldsymbol{x}, 0) + \triangle t^2 \boldsymbol{w}^0(\boldsymbol{x}), \tag{4.57}$$

where $\boldsymbol{w}^0$ is a bounded function.

4.2. Proof of Theorem 3.1. We first prove the following proposition.

PROPOSITION 4.1. *Let $\boldsymbol{u}^n$, $\boldsymbol{u}^*$, and p^n be the solution of* (4.1). *Let U^n, U^*, and P^n be the constructed approximate solution satisfying*

$$\begin{cases} \dfrac{U^* - U^n}{\triangle t} + (U^n \cdot \nabla)\, U^n = \Delta U^* + \triangle t^\alpha \ \boldsymbol{f}^n\,, \\ U^* = 0 \qquad on\ \partial\Omega\,, \\ \dfrac{U^{n+1} - U^*}{\triangle t} + \nabla P^n = \triangle t^\alpha \boldsymbol{g}^n\,, \\ \nabla \cdot U^{n+1} = 0\,, \\ \dfrac{\partial P^n}{\partial \boldsymbol{n}} = U^{n+1} \cdot \boldsymbol{n} = 0 \qquad on\ \partial\Omega\,, \\ U^0 = \boldsymbol{u}^0 + \triangle t^\alpha \ \boldsymbol{w}^0 \end{cases} \tag{4.58}$$

and

$$\max_{0\le n\le[\frac{T}{\Delta t}]+1} \|U^n(\cdot)\|_{W^{1,\infty}} \le C^*\,, \qquad \alpha > \tfrac{1}{2}\,. \tag{4.59}$$

Then for $0 \le t \le T$ *we have*

$$\|\boldsymbol{u}^n - U^n\|_{L^2} + \Delta t^{1/2}\left(\sum_n \|p^n - P^n\|^2_{H^1}\Delta t\right)^{1/2} \le C_1\ \Delta t^\alpha \tag{4.60}$$

and

$$\|\boldsymbol{u}^n - U^n\|_{L^\infty} + \Delta t\ \|p^n - P^n\|_{W^{1,\infty}} \le C_1\ \Delta t^{\alpha-1/2} \tag{4.61}$$

where

$$C_1 = C\ \|\boldsymbol{w}^0\|_{L^2} + C(C^*)\left(\sum_n \Delta t(\|\boldsymbol{f}^n\|^2_{L^2} + \|\boldsymbol{g}^n\|^2_{L^2} + \Delta t\|\boldsymbol{g}^n\|^2_{H^2})\right)^{1/2}. \tag{4.62}$$

Here C *and* C^* *are constants and* $n \le [\frac{T}{\Delta t}] + 1$.

Proof. Assume a priori that

$$\max_{0\le t^n\le T} \|\boldsymbol{u}^n\|_{L^\infty} \le \tilde{C}\,. \tag{4.63}$$

In the following estimates, the constant will sometimes depend on C^* and $\tilde{C}$. Later on we will estimate $\tilde{C}$.

Step 1. *Basic energy estimates.* Let

$$\boldsymbol{e}^n = U^n - \boldsymbol{u}^n\,, \qquad \boldsymbol{e}^* = U^* - \boldsymbol{u}^*\,, \qquad q^n = P^n - p^n\,. \tag{4.64}$$

Subtracting (4.58) from (4.1) we get the following error equation:

$$\begin{cases} \dfrac{\boldsymbol{e}^* - \boldsymbol{e}^n}{\Delta t} + (\boldsymbol{e}^n\cdot\nabla)\,U^n + (\boldsymbol{u}^n\cdot\nabla)\,\boldsymbol{e}^n = \Delta\boldsymbol{e}^* + \Delta t^\alpha \boldsymbol{f}^n\,, \\ \boldsymbol{e}^* = 0 \qquad \text{on } \partial\Omega\,, \\ \dfrac{\boldsymbol{e}^{n+1} - \boldsymbol{e}^*}{\Delta t} + \nabla q^n = \Delta t^\alpha \boldsymbol{g}^n\,, \\ \nabla\cdot\boldsymbol{e}^{n+1} = 0\,, \\ \dfrac{\partial q^n}{\partial \boldsymbol{n}} = \boldsymbol{e}^{n+1}\cdot\boldsymbol{n} = 0 \qquad \text{on } \partial\Omega\,, \\ \boldsymbol{e}^0 = \Delta t^\alpha\ \boldsymbol{w}^0\,. \end{cases} \tag{4.65}$$

Taking the scalar product of the first equation of (4.65) with $2e^*$ and integrating by parts, we obtain

$$\begin{aligned}
&\|e^*\|^2 - \|e^n\|^2 + \|e^* - e^n\|^2 + 2\Delta t\,\|\nabla e^*\|^2 \\
&\quad \le \Delta t^{2\alpha+1}\|f^n\|^2 + \Delta t\,\|e^*\|^2 \\
&\qquad -2\Delta t \int_\Omega e^*\cdot(e^n\cdot\nabla)\,U^n\,dx - 2\Delta t \int_\Omega e^*\cdot(u^n\cdot\nabla)\,e^n\,dx \\
&\quad \le \Delta t^{2\alpha+1}\|f^n\|^2 + \Delta t\,\|e^*\|^2 + C\,\Delta t\,\|e^*\|\,\|e^n\| \qquad (4.66)\\
&\qquad +2\Delta t \int_\Omega e^n\cdot(u^n\cdot\nabla)\,e^*\,dx \\
&\quad \le \Delta t^{2\alpha+1}\|f^n\|^2 + C^*\,\Delta t\,\|e^*\|^2 \\
&\qquad +(C^* + \tilde{C}^2)\,\Delta t\,\|e^n\|^2 + \Delta t\,\|\nabla e^*\|^2 .
\end{aligned}$$

Taking the scalar product of the second equation of (4.65) with $2e^{n+1}$ yields

$$\|e^{n+1}\|^2 - \|e^*\|^2 + \|e^{n+1} - e^*\|^2 \le \Delta t\,\|e^{n+1}\|^2 + \Delta t^{2\alpha+1}\|g^n\|^2 . \qquad (4.67)$$

Combining (4.66) and (4.67), we get

$$\begin{aligned}
&\|e^{n+1}\|^2 - \|e^n\|^2 + \|e^* - e^n\|^2 + \|e^{n+1} - e^*\|^2 + \Delta t\,\|\nabla e^*\|^2 \\
&\quad \le C\,\Delta t\,(\|e^{n+1}\|^2 + \|e^n\|^2) + \Delta t^{2\alpha+1}(\|f^n\|^2 + \|g^n\|^2) .
\end{aligned} \qquad (4.68)$$

Applying the discrete Gronwall lemma to the last inequality, we arrive at

$$\|e^n\| + \Delta t^{1/2}\,\|\nabla e^*\| + \left(\sum_n (\|e^* - e^n\|^2 + \|e^{n+1} - e^*\|^2)\right)^{1/2} \le C_1\Delta t^\alpha . \qquad (4.69)$$

Hence, from the second equation of (4.65), we have

$$\|e^n\| + \Delta t^{1/2}\left(\sum_n \|q^n\|_{H^1}^2\,\Delta t\right)^{1/2} \le C_1\Delta t^\alpha .$$

We have proved (4.60), assuming that $\tilde{C}$ in (4.63) is bounded independent of Δt.

Step 2. L^∞-*norm estimates.* Taking the divergence of the third equation of (4.65) we obtain

$$\begin{cases}
\Delta q^n = \dfrac{\nabla\cdot e^*}{\Delta t} - \Delta t^\alpha \nabla\cdot g^n , \\[2ex]
\dfrac{\partial q^n}{\partial n} = 0 \qquad \text{on } \partial\Omega .
\end{cases} \qquad (4.70)$$

Without loss of generality, we can normalize the pressure, such that $\int_\Omega q^n\,dx = 0$. Applying standard regularity theorems to the above Neumann problem, we arrive at

$$\|q^n\|_{H^2} \le C\,\Delta t^{-1}\|\nabla e^*\| + C\,\Delta t^\alpha\|g^n\|_{H^1} \le C_1\Delta t^{\alpha-3/2} . \qquad (4.71)$$

From the second equation in (4.65) we also have

$$\|\nabla e^{n+1}\| \le \|\nabla e^*\| + \Delta t\ \|q^n\|_{H^2} + \Delta t^{\alpha+1}\|g^n\|_{H^1} \le C_1\Delta t^{\alpha-1/2}\,. \tag{4.72}$$

From the first equation of (4.65) and (4.71), (4.72), we obtain

$$\|\Delta e^*\| \le \Delta t^{-1}\|e^* - e^n\| + C\left(\|e^n\| + \|\nabla e^n\| + \Delta t^{\alpha}\|f^n\|\right) \le C_1\Delta t^{\alpha-1}\,. \tag{4.73}$$

This implies

$$\|e^*\|_{H^2} \le C_1\Delta t^{\alpha-1}\,. \tag{4.74}$$

Using the Sobolev inequality, we get

$$\|e^*\|_{L^\infty} \le \|e^*\|^{1/2}\ \|e^*\|_{H^2}^{1/2} \le C_1\Delta t^{\alpha-1/2}\,. \tag{4.75}$$

From (4.70), we have

$$\|\Delta q^n\|_{H^1} \le \Delta t^{-1}\|e^*\|_{H^2} + \Delta t^{\alpha}\|g^n\|_{H^2} \le C_1\Delta t^{\alpha-2}\,. \tag{4.76}$$

This implies

$$\|q^n\|_{H^3} \le C_1\Delta t^{\alpha-2}\,. \tag{4.77}$$

Notice that the second equation of (4.65) gives

$$\|\nabla q^n\|_{L^2} \le \Delta t^{-1}\|e^{n+1} - e^*\| + \Delta t^{\alpha}\|g^n\|_{L^2} \le C_1\Delta t^{\alpha-1}\,. \tag{4.78}$$

Therefore with the Sobolev inequality, the Poincare inequality, and (4.77) we have

$$\|\nabla q^n\|_{L^\infty} \le \|\nabla q^n\|^{1/2}\ \|\nabla q^n\|_{H^2}^{1/2} \le C_1\Delta t^{\alpha-3/2}\,. \tag{4.79}$$

Using the second equation of (4.65) one more time, we get

$$\|e^{n+1}\|_{L^\infty} \le \|e^*\|_{L^\infty} + \Delta t\ \|\nabla q^n\|_{L^\infty} + \Delta t^{\alpha+1}\|g^n\|_{L^\infty} \le C_1\Delta t^{\alpha-1/2}\,. \tag{4.80}$$

Since $\alpha > \frac{1}{2}$, if we choose Δt small enough, we will always have

$$\|e^{n+1}\|_{L^\infty} \le 1\,. \tag{4.81}$$

Therefore in (4.63) we can choose

$$\tilde{C} = 1 + \max_{n\le 1+\left[\frac{T}{\Delta t}\right]} \|U^n(\cdot)\|_{L^\infty} \tag{4.82}$$

which depends only on the exact solution $(\boldsymbol{u}, p)$. This proves (4.61) and (4.62).

Proof of Theorem 3.1. Now, we simply use the above proposition and choose $N = 3$ in the expansion (4.49) to obtain

$$\|\boldsymbol{u}^n - U^n\|_{L^\infty(0,T;L^2)} + \Delta t^{1/2}\|p^n - P^n\|_{L^2(0,T;L^2)} \le C\Delta t. \tag{4.83}$$

But the boundary layer terms in P^n can be estimated as

$$\begin{aligned}
\|p(\cdot,t) - P^n\|_{L^2(0,T;L^2)} &\le \left(\sum_n \|\Delta t^{1/2}\varphi_1^n\|^2 \Delta t\right)^{1/2} \\
&= \Delta t \left(\sum_n \|\varphi_1^n\|^2\right)^{1/2} \\
&= \Delta t^{3/4} \left(\sum_n \|\partial_x p_0^n\|^2 \Delta t\right)^{1/2} \le C\Delta t^{3/4}.
\end{aligned} \tag{4.84}$$

Combining (4.83) and (4.84), we obtain (3.1). Clearly (3.3) is a direct consequence of Proposition 4.1.

Recall the expansion

$$p_{\triangle t}(\boldsymbol{x},t) = p_0(\boldsymbol{x},t) + \Delta t^{1/2}\partial_x p_0(-1,y,t)e^{-\xi} + O(\Delta t). \tag{4.85}$$

To get a uniform approximation for the pressure we need to subtract from $p_{\triangle t}$ the second term at the right-hand side. Note that this term involves p_0, which is not known. We need to approximate it by the numerical solution $p_{\triangle t}$. This can be done using (4.85) evaluated at $x = -1 + \Delta t^{1/2}$:

$$|\partial_x p_{\triangle t}(-1+\Delta t^{1/2}, y, t) - (1-e^{-1})\partial_x p_0(-1,y,t)| \le \Delta t^{1/2}. \tag{4.86}$$

Hence we get

$$p_{\triangle t}(\boldsymbol{x},t) = p_0(\boldsymbol{x},t) + \Delta t^{1/2}\frac{e}{e-1}\partial_x p_{\triangle t}(-1+\Delta t^{1/2},y,t)e^{-\xi} + O(\Delta t). \tag{4.87}$$

This proves (3.4).

5. Effects of numerical boundary conditions. In this section we focus on the issue that is the main source of confusion in the subject of projection methods: the boundary condition for pressure at the projection step. We will examine the effect of different boundary conditions on the accuracy of the numerical approximations using the explicit asymptotic analysis presented in the last section. As we have seen earlier, the Neumann boundary condition for pressure leads to numerical solutions with the following asymptotic form ($t = n\Delta t$):

$$\begin{aligned}
\boldsymbol{u}^n(\boldsymbol{x}) &= \boldsymbol{u}(\boldsymbol{x},t) + \Delta t\, \boldsymbol{u}_2(\boldsymbol{x},t) + \Delta t^2 \boldsymbol{u}_4 + \cdots, \\
\boldsymbol{u}^*(\boldsymbol{x}) &= \boldsymbol{u}(\boldsymbol{x},t) + \Delta t\,[\boldsymbol{u}_2^*(\boldsymbol{x},t,\Delta t) + \boldsymbol{a}_2^*((x\pm 1)/\Delta t^{1/2}, y, t)] + \cdots, \\
p^n(\boldsymbol{x}) &= p(\boldsymbol{x},t) + \Delta t^{1/2}\,\varphi_1((x\pm 1)/\Delta t^{1/2}, y, t) + \Delta t\, p_2(\boldsymbol{x},t) + \cdots.
\end{aligned} \tag{5.1}$$

We see that boundary layer terms of the order $\Delta t^{1/2}$ and Δt appear, respectively, in the pressure approximation and the intermediate velocity field, whereas the projected velocity field does not have numerical boundary layers.

Let us now replace the Neumann boundary condition (2.10) by a Dirichlet boundary condition:

$$\frac{\partial p^n}{\partial t} = 0 \quad \text{on } \partial\Omega, \tag{5.2}$$

or more specifically

$$p^n = 0 \quad \text{on } \partial\Omega . \tag{5.3}$$

To analyze the boundary layer structure of the resulting scheme, we proceed as in §4.1 and make the same ansatz as (4.2). Equations (4.7)–(4.16) remain valid. However, the boundary conditions are changed to

$$\boldsymbol{u}_0^* = 0, \quad p_0 + \varphi_0 = 0, \quad \text{at} \quad x = -1, \quad \xi = 0, \tag{5.4}$$

$$\boldsymbol{u}_j^* + \boldsymbol{a}_j^* = 0, \quad p_j + \varphi_j = 0, \quad \text{at} \quad x = -1, \quad \xi = 0, \tag{5.5}$$

for $j \geq 1$.

We still have (4.22) which, together with the boundary condition $\boldsymbol{u}_0 \,|_{\partial\Omega} = 0$ and the initial condition, determines $\boldsymbol{u}_0$ and p_0. This in turn gives the boundary condition for φ_0:

$$\varphi_0 \,|_{\xi=0} = -p_0 \,|_{x=-1} \,. \tag{5.6}$$

Going back to (4.20), we obtain

$$a_1^* = \partial_\xi \varphi_0 \,, \quad b_1^* = 0 \,, \tag{5.7}$$

$$\varphi_0(\xi, y, t) = -p_0(-1, y, t)\, e^{-\xi}. \tag{5.8}$$

Although $(\boldsymbol{u}_1, p_1)$ still satisfies the same equations (4.29), $\boldsymbol{u}_1$ no longer vanishes at the boundary. Instead, we have

$$(u_1, v_1)\,|_{x=-1} = (-\partial_\xi \varphi_0 \,|_{\xi=0}, 0) = (-p_0(-1, y, t), 0) \,. \tag{5.9}$$

This implies that, in general, we will have $(\boldsymbol{u}_1, p_1) \neq 0$. Therefore the numerical solution with the boundary condition (5.3) will have the following form ($t = n\triangle t$):

$$\begin{cases} \boldsymbol{u}^n(\boldsymbol{x}) = \boldsymbol{u}(\boldsymbol{x}, t) + \triangle t^{1/2} \boldsymbol{u}_1(\boldsymbol{x}, t) \, + \cdots, \\ \boldsymbol{u}^*(\boldsymbol{x}) = \boldsymbol{u}(\boldsymbol{x}, t) + \triangle t^{1/2} (\boldsymbol{u}_1^*(\boldsymbol{x}, t) + \boldsymbol{a}_1^*(\xi, y, t)) \, + \cdots, \\ p^n(\boldsymbol{x}) = p(\boldsymbol{x}, t) + \varphi_0(\xi, y, t) + \triangle t^{1/2} (p_1(\boldsymbol{x}, t) + \varphi_0(\xi, y, t)) \, + \cdots . \end{cases} \tag{5.10}$$

As a result of using the Dirichlet boundary condition (5.3), not only the accuracy of the pressure approximation deteriorates to order zero because of the appearance of $O(1)$ numerical boundary layer, the overall accuracy of the velocity approximation is also reduced to $O(\triangle t^{1/2})$. Note also that the leading-order error term in the velocity is not of boundary layer type. Clearly the boundary condition (5.3) is a bad choice.

A potentially better choice is suggested by (2.8):

$$\frac{\partial p^n}{\partial \boldsymbol{t}} = \boldsymbol{t} \cdot \Delta \boldsymbol{u}^n \qquad \text{on } \partial\Omega . \tag{5.11}$$

This may not be consistent since $\oint_{\partial\Omega} \frac{\partial p^n}{\partial \boldsymbol{t}} \, ds = 0$, whereas the line integral of $\boldsymbol{t} \cdot \Delta \boldsymbol{u}^n$ over $\partial\Omega$ may not be zero. Therefore we replace (5.11) by

$$\frac{\partial p^n}{\partial \boldsymbol{t}} = \boldsymbol{t} \cdot \Delta \boldsymbol{u}^n - \frac{1}{|\partial\Omega|} \int_{\partial\Omega} (\boldsymbol{t} \cdot \Delta \boldsymbol{u}^n) \, ds \qquad \text{on } \partial\Omega, \tag{5.12}$$

where $|\partial\Omega|$ denotes the total length of $\partial\Omega$. For the geometry we are considering, this becomes

$$\varphi^n(\pm 1, y, t) = \int_0^y \Delta v^n(\pm 1, z, t)\, dz - \frac{y}{2\pi}\int_0^{2\pi} \Delta v^n(\pm 1, z, t)\, dz \,. \tag{5.13}$$

To see the effect of this boundary condition, we follow the same procedure as described above. Again, (4.7)–(4.16) remain valid whereas (4.17)–(4.18) are changed to

$$\boldsymbol{u}_0^* = 0\,, \quad \boldsymbol{u}_j^* + \boldsymbol{a}_j^* = 0\,, \quad \text{at} \quad x = -1, \quad \xi = 0\,, \tag{5.14}$$

$$(p_j + \varphi_j)(-1, y, t) = \int_0^y \Delta v_j(-1, z, t)\, dz - \frac{y}{2\pi}\int_0^{2\pi} \Delta v_j(-1, z, t)\, dz\,, \tag{5.15}$$

for $j \geq 0$. The leading-order $(\boldsymbol{u}_0, p_0)$ still satisfies (4.22) which in turn determines the boundary condition for φ_0. Notice that at $x = -1$, (4.22) implies

$$\partial_y p_0 = \Delta v_0. \tag{5.16}$$

Consequently we have (from the periodicity in y)

$$\int_0^{2\pi} \Delta v_0(-1, y, t)\, dy = 0\,, \quad p_0(-1, y, t) = \int_0^y \Delta v_0(-1, z, t)\, dz\,. \tag{5.17}$$

Hence we obtain

$$\varphi_0 = 0, \quad \text{at} \quad \xi = 0\,. \tag{5.18}$$

Going back to (4.20), we get

$$\boldsymbol{a}_1^* = 0\,, \quad \varphi_0 = 0\,. \tag{5.19}$$

We now turn to the next-order terms. Obviously we still have

$$\boldsymbol{u}_1 = 0\,, \quad p_1 = 0\,. \tag{5.20}$$

Hence we get from (4.23), (4.24), and (5.15),

$$\varphi_1 = 0\,, \quad \boldsymbol{a}_2^* = 0\,. \tag{5.21}$$

The high-order terms will also be nonzero in general.

$$\varphi_2 \neq 0\,, \quad \boldsymbol{a}_3^* \neq 0\,, \tag{5.22}$$

We conclude that with the boundary condition (5.12) or (5.13), the numerical solutions take the following form ($t = n\Delta t$):

$$\begin{cases} \boldsymbol{u}^*(\boldsymbol{x}) = \boldsymbol{u}_0(\boldsymbol{x}, t) + \Delta t\ \boldsymbol{u}_2(\boldsymbol{x}, t) + O(\Delta t^{3/2})\,, \\ \boldsymbol{u}^n(\boldsymbol{x}) = \boldsymbol{u}_0(\boldsymbol{x}, t) + \Delta t\ \boldsymbol{u}_2(\boldsymbol{x}, t) + O(\Delta t^2)\,, \\ p^n(\boldsymbol{x}) = p_0(\boldsymbol{x}, t) + \Delta t\,[p_2(\boldsymbol{x}, t) + \varphi_2(\xi, y, t)] + O(\Delta t^{3/2})\,. \end{cases} \tag{5.23}$$

We see that the effect of (5.13) is to suppress the leading-order boundary layer terms in (5.1).

To obtain an improved Neumann boundary condition based on the first relation in (2.8), let us observe that p^n satisfies the Poisson equation

$$\Delta p^n = \frac{1}{\Delta t}\nabla\cdot\boldsymbol{u}^* \tag{5.24}$$

which implies

$$\int_{\partial\Omega}\frac{\partial p^n}{\partial \boldsymbol{n}}\,ds = -\frac{1}{\Delta t}\int_{\partial\Omega}\boldsymbol{u}^*\cdot\boldsymbol{n}\,ds = 0\,. \tag{5.25}$$

Direct imposition of

$$\frac{\partial p^n}{\partial \boldsymbol{n}} = \boldsymbol{n}\cdot\Delta\boldsymbol{u}^* \quad \text{or} \quad \boldsymbol{n}\cdot\Delta\boldsymbol{u}^n \qquad \text{on } \partial\Omega \tag{5.26}$$

may not be consistent with (5.25). However, since

$$\Delta\boldsymbol{u} = \nabla(\nabla\cdot\boldsymbol{u}) - \nabla\times(\nabla\times\boldsymbol{u}) \tag{5.27}$$

and $\nabla\cdot\boldsymbol{u}^n = 0$, $\nabla\cdot\boldsymbol{u}^* \sim 0$, we can use instead

$$\frac{\partial p^n}{\partial \boldsymbol{n}} = -\boldsymbol{n}\cdot[\nabla\times(\nabla\times\boldsymbol{u}^*)] \qquad \text{on } \partial\Omega \tag{5.28}$$

or

$$\frac{\partial p^n}{\partial \boldsymbol{n}} = -\boldsymbol{n}\cdot[\nabla\times(\nabla\times\boldsymbol{u}^n)] \qquad \text{on } \partial\Omega. \tag{5.29}$$

It is easy to check that both (5.28) and (5.29) are consistent with (5.25) and lead to (5.23). However, it remains an open question to rigorously justify these asymptotic statements.

6. Second-order schemes without spatial discretization. In this section we carry out the same program as in §4 for Kim and Moin's method (2.12). Again, we will concentrate on the time-discretized version and leave the fully discrete scheme to [10]. The second-order projection method with pressure increment formulation will be dealt with in a subsequent paper [9]. Analysis for the improved pressure boundary conditions still remains open.

6.1. Asymptotic analysis of Kim and Moin's method. Here we will leave out the nonlinear term since it does not affect the major steps but substantially complicates the presentation. The reader can readily fill in the missing terms when any standard second-order approximation of the nonlinear term is added in.

We begin with the following ansatz:

$$\begin{cases} \boldsymbol{u}^*(\boldsymbol{x}) = \boldsymbol{u}_0^*(\boldsymbol{x},t^n) + \sum\limits_{j=1} \varepsilon^j[\boldsymbol{u}_j^*(\boldsymbol{x},t^n) + \boldsymbol{a}_j^*(\xi,y,t^n)]\,, \\ \boldsymbol{u}^n(\boldsymbol{x}) = \boldsymbol{u}_0(\boldsymbol{x},t^n) + \sum\limits_{j=1} \varepsilon^j\boldsymbol{u}_j(\boldsymbol{x},t^n)\,, \\ p^{n-1/2}(\boldsymbol{x}) = p_0(\boldsymbol{x},t^{n-1/2}) + \sum\limits_{j=1} \varepsilon^j[p_j(\boldsymbol{x},t^{n-1/2}) + \varphi_j(\xi,y,t^{n-1/2})]\,. \end{cases} \tag{6.1}$$

Here again we set $\varepsilon = \triangle t^{1/2}$, $\xi = (x+1)/\varepsilon$, $t^n = n\triangle t$, $t^{n-1/2} = (n-\frac{1}{2})\triangle t$, $n = 1, 2, \ldots$. Substituting (6.1) into (2.12) and collecting equal powers of ε, we get the following equations.

From the first equation in (2.12), we get

$$\boldsymbol{u}_0^* = \boldsymbol{u}_0 \,, \tag{6.2}$$

$$\boldsymbol{u}_1^* + \boldsymbol{a}_1^* - \boldsymbol{u}_1 = \tfrac{1}{2}\partial_\xi^2 \boldsymbol{a}_1^* \,, \tag{6.3}$$

$$\boldsymbol{u}_2^* + \boldsymbol{a}_2^* - \boldsymbol{u}_2 = \tfrac{1}{2}(\Delta \boldsymbol{u}_0^* + \partial_\xi^2 \boldsymbol{a}_2^* + \Delta \boldsymbol{u}_0) \,. \tag{6.4}$$

For $j \geq 1$,

$$\boldsymbol{u}_{j+2}^* + \boldsymbol{a}_{j+2}^* - \boldsymbol{u}_{j+2} = \tfrac{1}{2}(\Delta \boldsymbol{u}_j^* + \partial_\xi^2 \boldsymbol{a}_{j+2}^* + \partial_y^2 \boldsymbol{a}_j^* + \Delta \boldsymbol{u}_j) \,. \tag{6.5}$$

From the third equation in (2.12), we get

$$\boldsymbol{u}_1^* + \boldsymbol{a}_1^* = \boldsymbol{u}_1 \,, \tag{6.6}$$

$$\boldsymbol{u}_2^* + \boldsymbol{a}_2^* = \boldsymbol{u}_2 + \partial_t \boldsymbol{u}_0 + \nabla p_0 + \nabla_\xi \varphi_1 \,, \tag{6.7}$$

$$\boldsymbol{u}_3^* + \boldsymbol{a}_3^* = \boldsymbol{u}_3 + \partial_t \boldsymbol{u}_1 + \nabla p_1 + \nabla_\xi \varphi_2 + \nabla_y \varphi_1 \,. \tag{6.8}$$

For $j = 2\ell, \ell \geq 1$,

$$\begin{aligned} \boldsymbol{u}_{j+2}^* + \boldsymbol{a}_{j+2}^* &= \boldsymbol{u}_{j+2} + \partial_t \boldsymbol{u}_j + \nabla p_j + \nabla_\xi \varphi_{j+1} + \nabla_y \varphi_j + \frac{1}{(\ell+1)!} \boldsymbol{u}_0^{(\ell+1)} \\ &\quad + \sum_{k=2}^{\ell} \frac{1}{k!} \boldsymbol{u}_{j-2k+2}^{(k)} + \frac{1}{2^\ell \ell!} \nabla p_0^{(\ell)} + \sum_{k=1}^{\ell-1} \frac{1}{2^k k!} \nabla p_{j-2k}^{(k)} \\ &\quad + \sum_{k=1}^{\ell} \frac{1}{2^k k!} (\nabla_\xi \varphi_{j-2k+1}^{(k)} + \nabla_y \varphi_{j-2k}^{(k)}) \,. \end{aligned} \tag{6.9}$$

For $j = 2\ell + 1, \ell \geq 1$,

$$\begin{aligned} \boldsymbol{u}_{j+2}^* + \boldsymbol{a}_{j+2}^* &= \boldsymbol{u}_{j+2} + \partial_t \boldsymbol{u}_j + \nabla p_j + \nabla_\xi \varphi_{j+1} + \nabla_y \varphi_j + \sum_{k=2}^{\ell+1} \frac{1}{k!} \boldsymbol{u}_{j-2k+2}^{(k)} \\ &\quad + \sum_{k=1}^{\ell} \frac{1}{2^k k!} (\nabla p_{j-2k}^{(k)} + \nabla_\xi \varphi_{j-2k+1}^{(k)} + \nabla_y \varphi_{j-2k}^{(k)}) \,. \end{aligned} \tag{6.10}$$

From the incompressibility condition, we get

$$\nabla \cdot \boldsymbol{u}^j = 0 \quad \text{for} \quad j \geq 0 \,. \tag{6.11}$$

The boundary conditions imply that for $x=-1$, $\xi=0$,

$$u_0 + u_0^* = 0\,, \tag{6.12}$$

$$u_1 + u_1^* + a_1^* = 0\,, \tag{6.13}$$

$$u_2 + u_2^* + a_2^* = \nabla p_0 + \nabla_\xi \varphi_1, \tag{6.14}$$

$$u_3 + u_3^* + a_3^* = \nabla p_1 + \nabla_\xi \varphi_2 + \nabla_y \varphi_1\,; \tag{6.15}$$

for $j = 2\ell$, $\ell \geq 2$,

$$\begin{aligned} u_j + u_j^* + a_j^* &= \nabla p_{j-2} + \nabla_\xi \varphi_{j-1} + \nabla_y \varphi_{j-2} \\ &\quad + \frac{(-1)^{\ell-1}}{2^{\ell-1}} \frac{1}{(\ell-1)!} \nabla p_0^{(\ell-1)} + \sum_{k=1}^{\ell-2} \frac{(-1)^k}{2^k k!} \nabla p_{j-2k-2}^{(k)} \\ &\quad + \sum_{k=1}^{\ell-1} \frac{(-1)^k}{2^k k!} (\nabla_\xi \varphi_{j-2k-1}^{(k)} + \nabla_y \varphi_{j-2k-2}^{(k)}); \end{aligned} \tag{6.16}$$

for $j = 2\ell+1$, $\ell \geq 2$,

$$\begin{aligned} u_j + u_j^* + a_j^* &= \nabla p_{j-2} + \nabla_\xi \varphi_{j-1} + \nabla_y \varphi_{j-2} \\ &\quad + \sum_{k=1}^{\ell-1} \frac{(-1)^k}{2^k k!} (\nabla p_{j-2k-2}^{(k)} + \nabla_\xi \varphi_{j-2k-1}^{(k)} + \nabla_y \varphi_{j-2k-2}^{(k)}); \end{aligned} \tag{6.17}$$

and for $j \geq 0$,

$$\partial_x p_j + \partial_\xi \varphi_{j+1} = 0\,. \tag{6.18}$$

Next we go through all these equations, order by order, to see if they are solvable. Since this is very similar to what we did in §4.1, we will only give a summary of the results.

The coefficients in the expansions (6.1) can be obtained successively in the following order:

$$u_0^*(x,t) = u_0(x,t)\,, \tag{6.19}$$

$$u_1^*(x,t) = u_1(x,t)\,, \tag{6.20}$$

$$a_1^* \equiv 0\,, \tag{6.21}$$

$$\left\{\begin{array}{l}\partial_t \boldsymbol{u}_0 + \nabla p_0 = \Delta \boldsymbol{u}_0\,, \\ \nabla\cdot \boldsymbol{u}_0 = 0\,, \\ \boldsymbol{u}_0 = 0 \qquad \text{on } \partial'\Omega\,, \end{array}\right. \tag{6.22}$$

$$\boldsymbol{u}_2^* = \boldsymbol{u}_2 + \partial_t \boldsymbol{u}_0 + \nabla p_0\,, \tag{6.23}$$

$$\left\{\begin{array}{l}\varphi_1 = \frac{1}{2}\partial_\xi^2 \varphi_1\,, \\ \partial_\xi \varphi_1 \mid_{\xi=0} \; = -\partial_x p_0 \mid_{x=-1}\,, \end{array}\right. \tag{6.24}$$

$$\varphi_1 = \frac{1}{\sqrt{2}}\partial_x p_0 \mid_{x=-1} e^{-\sqrt{2}\xi}\,, \tag{6.25}$$

$$a_2^* = \partial_\xi \varphi_1, \quad b_2^* = 0\,, \tag{6.26}$$

$$\left\{\begin{array}{l}\partial_t \boldsymbol{u}_1 + \nabla p_1 = \Delta \boldsymbol{u}_1\,, \\ \nabla\cdot \boldsymbol{u}_1 = 0\,, \\ \boldsymbol{u}_1 \mid_{\partial'\Omega} = 0\,, \quad \boldsymbol{u}_1(\boldsymbol{x},0) = 0\,. \end{array}\right. \tag{6.27}$$

This implies

$$\boldsymbol{u}_1 = 0\,, \quad p_1 = 0\,. \tag{6.28}$$

We next have

$$\boldsymbol{u}_3^* = \boldsymbol{u}_3\,, \tag{6.29}$$

$$\varphi_2 = 0\,, \quad a_3^* = 0\,, \quad b_3^* = \partial_y \varphi_1\,, \tag{6.30}$$

$$\left\{\begin{array}{l}\partial_t \boldsymbol{u}_2 + \nabla p_2 = \Delta \boldsymbol{u}_2 + \frac{1}{2}\Delta(\partial_t \boldsymbol{u}_0 + \nabla p_0) - \frac{1}{2}\partial_t^2 \boldsymbol{u}_0 - \frac{1}{2}\partial_t \nabla p_0\,, \\ \nabla\cdot \boldsymbol{u}_2 = 0\,, \\ \boldsymbol{u}_2 \mid_{\partial'\Omega} = 0\,, \quad \boldsymbol{u}_2(\boldsymbol{x},0) = 0\,. \end{array}\right. \tag{6.31}$$

This also implies

$$\boldsymbol{u}_2 = 0\,, \quad p_2 = 0\,, \tag{6.32}$$

$$\left\{\begin{array}{l}\varphi_3 = \frac{1}{2}(\partial_\xi^2 \varphi_3 + \partial_y^2 \varphi_1)\,, \\ \partial_\xi \varphi_3 \mid_{\xi=0} \; = 0\,, \end{array}\right. \tag{6.33}$$

$$\varphi_3(\xi, y, t) = \frac{1}{2}\partial_{xyy} p_0 \mid_{x=-1} \left(\frac{1}{\sqrt{2}} + \xi\right) \; e^{-\sqrt{2}\xi}\,, \tag{6.34}$$

$$a_4^* = \partial_\xi \varphi_3 + \frac{1}{2}\partial_\xi \varphi_1^{(1)}\,, \quad b_4^* = 0\,, \tag{6.35}$$

$$u_4^* = u_4 + \tfrac{1}{2}u_0^{(2)} + \tfrac{1}{2}\nabla p_0^{(1)}, \tag{6.36}$$

$$u_3 = 0, \quad p_3 = 0, \tag{6.37}$$

$$\varphi_4 = 0, \quad a_5^* = 0, \quad b_5^* = \partial_y\varphi_3 + \tfrac{1}{2}\partial_y\varphi_1^{(1)}, \tag{6.38}$$

$$u_5^* = u_5, \tag{6.39}$$

$$\begin{cases} \partial_t u_4 + \nabla p_4 = \Delta u_4 + \tfrac{1}{4}\Delta(u_0^{(2)} + \nabla p_0^{(1)}) - \tfrac{1}{6}u_0^{(3)} - \tfrac{1}{8}\nabla p_0^{(2)}, \\ \nabla\cdot u_4 = 0, \\ u_4\,|_{x=-1} = -\tfrac{1}{2}\partial_t(\nabla p_0 + \tfrac{1}{2}\nabla_\xi\varphi_1)\,|_{x=-1,\xi=0}\,. \end{cases} \tag{6.40}$$

In the last equation, there is a similar boundary condition at $x = 1$. With suitable initial data, (6.40) has a smooth solution. Again we will defer the discussions on choosing the initial data until the end of this subsection.

Continuing in this fashion, we obtain

$$\begin{cases} \varphi_5 = \tfrac{1}{2}(\partial_\xi^2\varphi_5 + \partial_y^2\varphi_3), \\ \partial_\xi\varphi_5\,|_{\xi=0} = -\partial_x p_4\,|_{x=-1}, \end{cases} \tag{6.41}$$

$$a_6^* = \partial_\xi\varphi_5 + \tfrac{1}{2}\partial_\xi\partial_t\varphi_3, \quad b_6^* = 0, \tag{6.42}$$

$$u_6^* = u_6 + u_4^{(1)} + \tfrac{1}{6}u_0^{(3)} + \nabla p_4 + \tfrac{1}{8}\nabla p_0^{(2)}, \tag{6.43}$$

$$\begin{cases} \partial_t u_5 + \nabla p_5 = \Delta u_5, \\ \nabla\cdot u_5 = 0, \\ u_5\,|_{x=-1} = -\tfrac{1}{2}\partial_t\nabla_y\varphi_1\,|_{x=-1,\xi=0}\,. \end{cases} \tag{6.44}$$

Notice that as in the case of the first-order scheme, we generally have $(u_5, p_5) \neq 0$, because of the contributions from the boundary. We have

$$\begin{cases} \varphi_6 = \tfrac{1}{2}(\partial_\xi^2\varphi_6 + \partial_y^2\varphi_4), \\ \partial_\xi\varphi_6\,|_{\xi=0} = -\partial_x p_5\,|_{x=-1}, \end{cases} \tag{6.45}$$

$$a_7^* = \partial_\xi\varphi_6, \quad b_7^* = \partial_y\varphi_5 + \tfrac{1}{2}\partial_y\varphi_3^{(1)}, \tag{6.46}$$

$$u_7^* = u_7 + \partial_t u_5 + \nabla p_5, \tag{6.47}$$

$$\begin{cases} \partial_t u_6 + \nabla p_6 = \Delta u_6 + \dfrac{1}{2}\Delta(\partial_t u_4 + \nabla p_4 + \dfrac{1}{6}u_0^{(3)} + \dfrac{1}{8}\nabla p_0^{(2)}) \\ \qquad\qquad -\dfrac{1}{4!}u_0^{(4)} - \dfrac{1}{2}u_4^{(2)} - \dfrac{1}{2^3 3!}\nabla p_0^{(3)} - \nabla p_4^{(1)}, \\ \nabla\cdot u_6 = 0, \\ u_6\,|_{x=-1} = \dfrac{1}{4}\nabla p_0^{(2)}\,|_{x=-1} - \dfrac{1}{8}\nabla_\xi\varphi_1^{(2)}\,|_{\xi=0}, \end{cases} \tag{6.48}$$

$$\left\{\begin{array}{l}\varphi_7 = \frac{1}{2}(\partial_\xi^2\varphi_7 + \partial_y^2\varphi_5)\,,\\ \partial_\xi\varphi_7\,|_{\xi=0} = -\partial_x p_6\,|_{x=-1}\,,\end{array}\right. \tag{6.49}$$

$$a_8^* = \sum_{k=0}^{3}\frac{1}{2^k k!}\partial_\xi\varphi_{j-2k}^{(k)}\,, \quad b_8^* = \partial_y\varphi_6\,, \tag{6.50}$$

$$\boldsymbol{u}_8^* = \boldsymbol{u}_8 + \boldsymbol{u}_6^{(1)} + \frac{1}{2}\boldsymbol{u}_4^{(2)} + \frac{1}{4!}\boldsymbol{u}_0^{(4)} + \nabla p_6 + \frac{1}{2}\nabla p_4^{(1)} + \frac{1}{48}\nabla p_0^{(3)}\,, \tag{6.51}$$

$$\left\{\begin{array}{l}\partial_t\boldsymbol{u}_7 + \nabla p_7 = \Delta\boldsymbol{u}_7 + \frac{1}{2}\Delta(\partial_t\boldsymbol{u}_5 + \nabla p_5) - \frac{1}{2}\boldsymbol{u}_5^{(2)} - \frac{1}{2}\nabla p_5^{(1)}\,,\\ \nabla\cdot\boldsymbol{u}_7 = 0\,,\\ \boldsymbol{u}_7\,|_{x=-1} = -\frac{1}{2}\nabla_y(\varphi_5 - \varphi_3^{(1)} + \frac{5}{8}\varphi_1^{(2)})\,|_{x=-1,\xi=0}\,.\end{array}\right. \tag{6.52}$$

In general, if we let

$$\psi_j = \sum_{k=0}^{[j/2]}\frac{1}{2^k k!}\varphi_{j-2k}^{(k)} = \varphi_j + \frac{1}{2}\partial_t\varphi_{j-2} + \frac{1}{8}\partial_t^2\varphi_{j-4} + \cdots \tag{6.53}$$

such that $\{\varphi_j\}_{j\geq 4}$ satisfies

$$\left\{\begin{array}{l}\varphi_j = \frac{1}{2}(\partial_\xi^2\varphi_j + \partial_y^2\varphi_{j-2})\,,\\ \partial_\xi\varphi_j\,|_{\xi=0} = -\partial_x p_{j-1}\,|_{x=-1}\end{array}\right. \tag{6.54}$$

and φ_j decays exponentially as $\xi \to +\infty$, then we have

$$a_j^* = \partial_\xi\psi_{j-1}\,, \quad b_j^* = \partial_y\psi_{j-2}\,. \tag{6.55}$$

Clearly $\boldsymbol{a}_j^*$ also decays exponentially as $\xi \to +\infty$. On the other hand, $(\boldsymbol{u}_j, p_j)$ solves a system of linear Stokes equations with source terms.

Now if we let

$$\left\{\begin{array}{l}U^* = \boldsymbol{u}_0 + \displaystyle\sum_{j=1}^{2N}\varepsilon^j(\boldsymbol{u}_j^* + \boldsymbol{a}_j^*)\,,\\ U^n = \boldsymbol{u}_0 + \displaystyle\sum_{j=1}^{2N}\varepsilon^j\boldsymbol{u}_j\,,\\ P^{n-1/2} = p_0 + \displaystyle\sum_{j=1}^{2N}\varepsilon^j(p_j + \varphi_j) + \varepsilon^{2N+1}\varphi_{2N+1}\,,\end{array}\right. \tag{6.56}$$

then we have

$$\left\{\begin{array}{ll}\dfrac{U^* - U^n}{\Delta t} = \Delta\dfrac{U^* + U^n}{2} + \Delta t^{N-1/2}\boldsymbol{f}_N\,, & \\ U^* + U^n = \Delta t\nabla P^{n-1/2} & \text{on } \partial\Omega\,,\\ U^* = U^{n+1} + \Delta t\nabla P^{n+1/2} + \Delta t^{N+1/2}\boldsymbol{g}_N\,, & \\ \nabla\cdot U^{n+1} = 0\,, & \\ \dfrac{\partial(P^{n+1/2} - P^{n-1/2})}{\partial\boldsymbol{n}} = \boldsymbol{n}\cdot U^{n+1} = 0 & \text{on } \partial\Omega,\end{array}\right. \tag{6.57}$$

where $\boldsymbol{f}_N$, $\boldsymbol{g}_N$ are bounded and smooth if $(\boldsymbol{u}_0, p_0)$ is sufficiently smooth.

As in §4.1, if we do not assume any compatibility condition for u^0, then the smoothness of $(\boldsymbol{u}_4, p_4)$ at $t = 0$ requires us to choose initial data for (6.40) such that it matches the boundary condition in (6.40). This restricts the approximation at $t = 0$ to

$$U^0(\boldsymbol{x}) = \boldsymbol{u}^0(\boldsymbol{x}) + \Delta t^2 \boldsymbol{w}^0(\boldsymbol{x}), \tag{6.58}$$

where $\boldsymbol{w}^0$ is a bounded function.

However, it is straightforward to check that under the compatibility conditions stated in Theorem 3.2, we can choose

$$\boldsymbol{u}_4(\boldsymbol{x}, 0) = \boldsymbol{u}_5(\boldsymbol{x}, 0) = \boldsymbol{u}_6(\boldsymbol{x}, 0) = \boldsymbol{u}_7(\boldsymbol{x}, 0) = 0. \tag{6.59}$$

Consequently, we have

$$U^0(\boldsymbol{x}) = \boldsymbol{u}^0(\boldsymbol{x}) + \Delta t^4 \boldsymbol{w}^0(\boldsymbol{x}), \tag{6.60}$$

where $\boldsymbol{w}^0$ is a bounded function.

6.2. Proof of Theorem 3.2. As in the proof of Theorem 3.1, Theorem 3.2 is a direct consequence of the following result, together with (6.56) with $N = 5$.

PROPOSITION 6.1. *Let $\boldsymbol{u}^n$, $\boldsymbol{u}^*$, and p^n be the solution of* (2.12) *with initial data $\boldsymbol{u}^0$. Let U^n, U^*, and P^n be the constructed approximate solution satisfying*

$$\left\{ \begin{aligned} & \frac{U^* - U^n}{\Delta t} = \Delta \frac{U^* + U^n}{2} - \frac{3}{2}(U^n \cdot \nabla)\, U^n + \frac{1}{2}(U^{n-1} \cdot \nabla)\, U^{n-1} + \Delta t^\alpha \boldsymbol{f}^n, \\ & U^* + U^n = \Delta t\, \nabla P^{n-1/2} \qquad on\ \partial\Omega, \\ & \frac{U^{n+1} - U^*}{\Delta t} + \nabla P^{n+1/2} = \Delta t^\alpha \boldsymbol{g}^n, \\ & \nabla \cdot U^{n+1} = 0, \\ & \frac{\partial (P^{n+1/2} - P^{n-1/2})}{\partial \boldsymbol{n}} = \boldsymbol{n} \cdot U^{n+1} = 0 \qquad on\ \partial\Omega, \\ & U^0 = \boldsymbol{u}^0 + \Delta t^\alpha \boldsymbol{w}^0 \end{aligned} \right. \tag{6.61}$$

and

$$\max_{0 \le n \le [\frac{T}{\Delta t}]+1} \|U^n(\cdot)\|_{W^{1,\infty}} \le C^*, \qquad \alpha > \tfrac{7}{4}. \tag{6.62}$$

Then we have

$$\|\boldsymbol{u}^n - U^n\|_{L^2} + \Delta t\, \|p^n - P^n\|_{H^1} \le C_1 \Delta t^\alpha \tag{6.63}$$

and

$$\|\boldsymbol{u}^n - U^n\|_{L^\infty} + \Delta t\, \|p^n - P^n\|_{W^{1,\infty}} \le C_1 \Delta t^{\alpha - 7/4}, \tag{6.64}$$

where C_1 is the same as in Proposition 4.1.

Proof. As in the proof of Proposition 4.1, we assume a priori that

$$\|\boldsymbol{u}^n\|_{L^\infty} \le \tilde{C} \tag{6.65}$$

for $n \le [\frac{T}{\Delta t}] + 1$.

Step 1. *Equation for error functions.* We first reformulate Kim and Moin's scheme (2.12) by introducing the new intermediate variables $\hat{\boldsymbol{u}}^*, \hat{U}^*$:

$$\begin{aligned} &\boldsymbol{u}^* + \boldsymbol{u}^n - \Delta t \ \nabla p^{n-1/2} = 2\hat{\boldsymbol{u}}^* \,, \\ &U^* + U^n - \Delta t \ \nabla P^{n-1/2} = 2\hat{U}^* \,. \end{aligned} \tag{6.66}$$

(2.12) becomes

$$\left\{ \begin{aligned} &\frac{2(\hat{\boldsymbol{u}}^* - \boldsymbol{u}^n)}{\Delta t} + \nabla \left(p^{n-1/2} - \frac{1}{2}\Delta t \ \Delta p^{n-1/2} \right) \\ &\qquad = \Delta \hat{\boldsymbol{u}}^* - \frac{3}{2}(\boldsymbol{u}^n \!\cdot\! \nabla) \ \boldsymbol{u}^n + \frac{1}{2}(\boldsymbol{u}^{n-1} \!\cdot\! \nabla) \ \boldsymbol{u}^{n-1} \,, \\ &\hat{\boldsymbol{u}}^* = 0 \quad \text{on } \partial\Omega \,, \\ &\frac{\boldsymbol{u}^{n+1} + \boldsymbol{u}^n - 2\hat{\boldsymbol{u}}^*}{\Delta t} + \nabla(p^{n+1/2} - p^{n-1/2}) = 0 \,, \\ &\nabla \!\cdot\! \boldsymbol{u}^{n+1} = 0 \,, \\ &\boldsymbol{u}^{n+1} \!\cdot\! \boldsymbol{n} = 0 \quad \text{on } \partial\Omega \,. \end{aligned} \right. \tag{6.67}$$

The approximate solution (6.57) changes similarly. Let

$$\boldsymbol{e}^n = U^n - \boldsymbol{u}^n \,, \qquad \boldsymbol{e}^* = \hat{U}^* - \hat{\boldsymbol{u}}^* \,, \qquad q^n = P^{n-1/2} - p^{n-1/2} \,. \tag{6.68}$$

Subtracting the reformulated form of (6.57) from (6.67), we get an equation for the error functions:

$$\left\{ \begin{aligned} &\frac{2(\boldsymbol{e}^* - \boldsymbol{e}^n)}{\Delta t} + \nabla \left(q^n - \frac{1}{2}\Delta t \ \Delta q^n \right) = \Delta \boldsymbol{e}^* + \frac{1}{2}(\boldsymbol{e}^{n-1} \!\cdot\! \nabla) \ U^{n-1} \\ &\qquad + \frac{1}{2}(\boldsymbol{u}^{n-1} \!\cdot\! \nabla) \ \boldsymbol{e}^{n-1} - \frac{3}{2}(\boldsymbol{e}^n \!\cdot\! \nabla) \ U^n - \frac{3}{2}(\boldsymbol{u}^n \!\cdot\! \nabla) \ \boldsymbol{e}^n + \Delta t^\alpha \boldsymbol{f}^n \,, \\ &\boldsymbol{e}^* = 0 \quad \text{on } \partial\Omega \,, \\ &\frac{\boldsymbol{e}^{n+1} + \boldsymbol{e}^n - 2\boldsymbol{e}^*}{\Delta t} + \nabla(q^{n+1} - q^n) = \Delta t^\alpha \boldsymbol{g}^n \,, \\ &\nabla \!\cdot\! \boldsymbol{e}^{n+1} = 0 \,, \\ &\frac{\partial(q^{n+1} - q^n)}{\partial \boldsymbol{n}} = \boldsymbol{e}^{n+1} \!\cdot\! \boldsymbol{n} = 0 \quad \text{on } \partial\Omega \,, \\ &\boldsymbol{e}^0 = \Delta t^\alpha \boldsymbol{w}^0 \,. \end{aligned} \right. \tag{6.69}$$

Step 2. *Basic energy estimate.* Taking the scalar product of the first equation of (6.69) with $\boldsymbol{e}^*$ and integrating by parts, we get

$$\begin{aligned} &\|\boldsymbol{e}^*\|^2 - \|\boldsymbol{e}^n\|^2 + \|\boldsymbol{e}^* - \boldsymbol{e}^n\|^2 + \Delta t \ \|\nabla \boldsymbol{e}^*\|^2 \\ &\quad \le -\Delta t \int_\Omega \boldsymbol{e}^* \!\cdot\! \nabla \left(q^n - \frac{1}{2}\Delta t \Delta q^n \right) \, d\boldsymbol{x} + C \, \Delta t^{2\alpha+1} \|\boldsymbol{f}^n\|^2 \\ &\qquad + C \, \Delta t \ (\|\boldsymbol{e}^n\|^2 + \|\boldsymbol{e}^{n-1}\|^2 + \|\boldsymbol{e}^*\|^2) + \frac{1}{4}\Delta t \ \|\nabla \boldsymbol{e}^*\|^2 \,. \end{aligned} \tag{6.70}$$

Taking the scalar product of the second equation of (6.69) with $\boldsymbol{e}^{n+1}$, we obtain

$$
\begin{aligned}
&\|\boldsymbol{e}^{n+1}\|^2 - \|\boldsymbol{e}^*\|^2 + \|\boldsymbol{e}^{n+1} - \boldsymbol{e}^*\|^2 \\
&\quad -\tfrac{1}{2}(\|\boldsymbol{e}^{n+1}\|^2 - \|\boldsymbol{e}^n\|^2) - \tfrac{1}{2}\|\boldsymbol{e}^{n+1} - \boldsymbol{e}^n\|^2 \\
&\le C\,\Delta t^{2\alpha+1}\|\boldsymbol{g}^n\|^2 + C\,\Delta t\;\|\boldsymbol{e}^{n+1}\|^2 .
\end{aligned} \tag{6.71}
$$

Combining these two estimates we obtain

$$
\begin{aligned}
&\frac{1}{2}(\|\boldsymbol{e}^{n+1}\|^2 - \|\boldsymbol{e}^n\|^2) + \|\boldsymbol{e}^* - \boldsymbol{e}^n\|^2 + \|\boldsymbol{e}^{n+1} - \boldsymbol{e}^*\|^2 \\
&\quad -\frac{1}{2}\|\boldsymbol{e}^{n+1} - \boldsymbol{e}^n\|^2 + \frac{3}{4}\Delta t\;\|\nabla \boldsymbol{e}^*\|^2 \\
&\le -\Delta t \int_\Omega \boldsymbol{e}^*\cdot\nabla\left(q^n - \frac{1}{2}\Delta t\Delta q^n\right)\,d\boldsymbol{x} + C\,\Delta t^{2\alpha+1}(\|\boldsymbol{f}^n\|^2 + \|\boldsymbol{g}^n\|^2) \\
&\quad +C\,\Delta t\;(\|\boldsymbol{e}^n\|^2 + \|\boldsymbol{e}^{n-1}\|^2 + \|\boldsymbol{e}^*\|^2 + \|\boldsymbol{e}^{n+1}\|^2) .
\end{aligned} \tag{6.72}
$$

Since

$$
2\|\boldsymbol{e}^* - \boldsymbol{e}^n\|^2 + 2\|\boldsymbol{e}^{n+1} - \boldsymbol{e}^*\|^2 = \|\boldsymbol{e}^{n+1} - \boldsymbol{e}^n\|^2 + \|\boldsymbol{e}^{n+1} + \boldsymbol{e}^n - 2\boldsymbol{e}^*\|^2 , \tag{6.73}
$$

we get

$$
\begin{aligned}
&\|\boldsymbol{e}^{n+1}\|^2 - \|\boldsymbol{e}^n\|^2 + \|\boldsymbol{e}^{n+1} + \boldsymbol{e}^n - 2\boldsymbol{e}^*\|^2 + \frac{3}{2}\Delta t\;\|\nabla \boldsymbol{e}^*\|^2 \\
&\le -2\Delta t \int_\Omega \boldsymbol{e}^*\cdot\nabla\left(q^n - \frac{1}{2}\Delta t\Delta q^n\right)\,d\boldsymbol{x} \\
&\quad +C\,\Delta t\;(\|\boldsymbol{e}^n\|^2 + \|\boldsymbol{e}^{n-1}\|^2 + \|\boldsymbol{e}^{n+1}\|^2) \\
&\quad +C\,\Delta t^{2\alpha+1}(\|\boldsymbol{f}^n\|^2 + \|\boldsymbol{g}^n\|^2) .
\end{aligned} \tag{6.74}
$$

To estimate the first term on the right-hand side of (6.74), we let

$$
\begin{aligned}
I &\equiv -2\Delta t \int_\Omega \boldsymbol{e}^*\cdot\nabla\left(q^n - \frac{1}{2}\Delta t\;\Delta q^n\right)\,d\boldsymbol{x} \\
&= -2\Delta t \int_\Omega \boldsymbol{e}^*\cdot\nabla q^n\,d\boldsymbol{x} - \Delta t^2 \int_\Omega (\nabla\cdot\boldsymbol{e}^*)\Delta q^n\,d\boldsymbol{x} \equiv I_1 + I_2 .
\end{aligned} \tag{6.75}
$$

Using the second equation in (6.69) and integrating by parts, we can write the first term as

$$
\begin{aligned}
I_1 &= -2\Delta t \int_\Omega \boldsymbol{e}^*\cdot\nabla q^n\,d\boldsymbol{x} \\
&= -\Delta t^2 \int_\Omega \nabla(q^{n+1} - q^n)\nabla q^n\,d\boldsymbol{x} - \Delta t^{\alpha+2}\int_\Omega \boldsymbol{g}^n\cdot\nabla q^n\,d\boldsymbol{x} \\
&= -\frac{1}{2}\Delta t^2(\|\nabla q^{n+1}\|^2 - \|\nabla q^n\|^2) \\
&\quad +\frac{1}{2}\Delta t^2\|\nabla(q^{n+1} - q^n)\|^2 - \Delta t^{\alpha+2}\int_\Omega \boldsymbol{g}^n\cdot\nabla q^n\,d\boldsymbol{x} .
\end{aligned} \tag{6.76}
$$

Since

$$
\begin{aligned}
\frac{1}{2}\Delta t^2\|\nabla(q^{n+1}-q^n)\|^2 &= \frac{1}{2}\|\boldsymbol{e}^{n+1}+\boldsymbol{e}^n-2\boldsymbol{e}^*\|^2 \\
&+\frac{1}{2}\Delta t^{2\alpha+2}\|\boldsymbol{g}^n\|^2+\Delta t^{\alpha+1}\int_\Omega \boldsymbol{g}^n\cdot(\boldsymbol{e}^{n+1}+\boldsymbol{e}^n-2\boldsymbol{e}^*)\,d\boldsymbol{x}\,,
\end{aligned}
\tag{6.77}
$$

we have

$$
\begin{aligned}
I_1 &= -\frac{1}{2}\Delta t^2(\|\nabla q^{n+1}\|^2-\|\nabla q^n\|^2)+\frac{1}{2}\|\boldsymbol{e}^{n+1}+\boldsymbol{e}^n-2\boldsymbol{e}^*\|^2+\frac{1}{2}\Delta t^{2\alpha+2}\|\boldsymbol{g}^n\|^2 \\
&+\Delta t^{\alpha+1}\int_\Omega \boldsymbol{g}^n\cdot(\boldsymbol{e}^{n+1}+\boldsymbol{e}^n-2\boldsymbol{e}^*)\,d\boldsymbol{x}-\Delta t^{\alpha+2}\int_\Omega \boldsymbol{g}^n\cdot\nabla q^n\,d\boldsymbol{x}\,.
\end{aligned}
\tag{6.78}
$$

Next we rewrite the second term as

$$
\begin{aligned}
I_2 &= -\Delta t^2\int_\Omega(\nabla\cdot\boldsymbol{e}^*)\Delta q^n\,d\boldsymbol{x} \\
&= -\frac{1}{2}\Delta t^3\int_\Omega \Delta(q^{n+1}-q^n)\Delta q^n\,d\boldsymbol{x}-\frac{1}{2}\Delta t^{\alpha+3}\int_\Omega(\nabla\cdot\boldsymbol{g}^n)\Delta q^n\,d\boldsymbol{x} \\
&= -\frac{1}{4}\Delta t^3(\|\Delta q^{n+1}\|^2-\|\Delta q^n\|^2)+\frac{1}{4}\Delta t^3\|\Delta(q^{n+1}-q^n)\|^2 \\
&\quad -\frac{1}{2}\Delta t^{\alpha+3}\int_\Omega(\nabla\cdot\boldsymbol{g}^n)\Delta q^n\,d\boldsymbol{x} \\
&= -\frac{1}{4}\Delta t^3(\|\Delta q^{n+1}\|^2-\|\Delta q^n\|^2)+\Delta t\,\|\nabla\cdot\boldsymbol{e}^*\|^2+\frac{1}{4}\Delta t^{2\alpha+3}\|\nabla\cdot\boldsymbol{g}^n\|^2 \\
&\quad -\Delta t^{\alpha+2}\int_\Omega(\nabla\cdot\boldsymbol{g}^n)(\nabla\cdot\boldsymbol{e}^*)\,d\boldsymbol{x}-\frac{1}{2}\Delta t^{\alpha+3}\int_\Omega(\nabla\cdot\boldsymbol{g}^n)\Delta q^n\,d\boldsymbol{x}\,.
\end{aligned}
\tag{6.79}
$$

Combining these two terms we arrive at

$$
\begin{aligned}
I &= -\frac{1}{2}\Delta t^2(\|\nabla q^{n+1}\|^2-\|\nabla q^n\|^2)-\frac{1}{4}\Delta t^3(\|\Delta q^{n+1}\|^2-\|\Delta q^n\|^2) \\
&\quad +\frac{1}{2}\|\boldsymbol{e}^{n+1}+\boldsymbol{e}^n-2\boldsymbol{e}^*\|^2+\Delta t\,\|\nabla\cdot\boldsymbol{e}^*\|^2 \\
&\quad +\Delta t^{\alpha+1}\int_\Omega \boldsymbol{g}^n\cdot(\boldsymbol{e}^{n+1}+\boldsymbol{e}^n-2\boldsymbol{e}^*)\,d\boldsymbol{x}-\Delta t^{\alpha+2}\int_\Omega \boldsymbol{g}^n\cdot\nabla q^n\,d\boldsymbol{x} \\
&\quad -\Delta t^{\alpha+2}\int_\Omega(\nabla\cdot\boldsymbol{g}^n)(\nabla\cdot\boldsymbol{e}^*)\,d\boldsymbol{x}-\frac{1}{2}\Delta t^{\alpha+3}\int_\Omega(\nabla\cdot\boldsymbol{g}^n)\Delta q^n\,d\boldsymbol{x} \\
&\quad +\frac{1}{4}\Delta t^{2\alpha+3}\|\nabla\cdot\boldsymbol{g}^n\|^2+\frac{1}{2}\|\Delta t^{\alpha+1}\boldsymbol{g}^n\|^2\,.
\end{aligned}
\tag{6.80}
$$

This gives

$$
\begin{aligned}
I &\le -\tfrac{1}{2}\Delta t^2(\|\nabla q^{n+1}\|^2-\|\nabla q^n\|^2)-\tfrac{1}{4}\Delta t^3(\|\Delta q^{n+1}\|^2-\|\Delta q^n\|^2) \\
&\quad +\tfrac{1}{2}\|\boldsymbol{e}^{n+1}+\boldsymbol{e}^n-2\boldsymbol{e}^*\|^2+\Delta t\,\|\nabla\boldsymbol{e}^*\|^2+\Delta t\|\boldsymbol{e}^{n+1}+\boldsymbol{e}^n-2\boldsymbol{e}^*\|^2 \\
&\quad +2\Delta t^3\|\nabla q^n\|^2+2\Delta t^4\|\Delta q^n\|^2+2\Delta t^{2\alpha+1}(\|\boldsymbol{g}^n\|^2+\Delta t\|\boldsymbol{g}^n\|^2_{H^1})\,.
\end{aligned}
\tag{6.81}
$$

Going back to (6.74) we obtain

$$
\begin{aligned}
&\|e^{n+1}\|^2 - \|e^n\|^2 + \tfrac{1}{2}\|e^{n+1} + e^n - 2e^*\|^2 + \tfrac{1}{2}\Delta t\,\|\nabla e^*\|^2 \\
&\quad + \tfrac{1}{2}\Delta t^2(\|\nabla q^{n+1}\|^2 - \|\nabla q^n\|^2) + \tfrac{1}{4}\Delta t^3(\|\Delta q^{n+1}\|^2 - \|\Delta q^n\|^2) \\
&\quad \le \Delta t^3\|\nabla q^n\|^2 + \Delta t^4\|\Delta q^n\|^2 + C\,\Delta t\,(\|e^n\|^2 + \|e^{n-1}\|^2 + \|e^{n+1}\|^2) \\
&\quad + C\,\Delta t^{2\alpha+1}(\|f^n\|^2 + \Delta t\|g^n\|^2_{H^1}).
\end{aligned}
\tag{6.82}
$$

Gronwall's inequality gives

$$
\|e^n\| + \|e^*\| + \Delta t\,\|\nabla q^n\| + \Delta t^{3/2}\,\|\Delta q^n\| + \Delta t^{1/2}\|\nabla e^*\| \le C_1\Delta t^\alpha . \tag{6.83}
$$

Step 3. *L^∞-norm estimate.* Taking the divergence of the second equation in (6.69), we obtain

$$
\begin{cases}
\Delta(q^{n+1} - q^n) = 2\dfrac{\nabla\cdot e^*}{\Delta t} + \Delta t^\alpha \nabla\cdot g^n , \\[2ex]
\dfrac{\partial(q^{n+1} - q^n)}{\partial n} = 0 \qquad \text{on } \partial'\Omega .
\end{cases}
\tag{6.84}
$$

We can always normalize pressure such that $\int_\Omega (q^{n+1} - q^n)\,dx = 0$. Applying the standard regularity theorem to (6.84) and using (6.83), we have

$$
\|q^{n+1} - q^n\|_{H^2} \le C\,\|\Delta(q^{n+1} - q^n)\| \le C\Delta t^{\alpha-3/2} . \tag{6.85}
$$

The second equation of (6.69) implies directly

$$
\begin{aligned}
\|\nabla(e^{n+1} + e^n)\| &\le 2\|\nabla e^*\| + \Delta t\|q^{n+1} - q^n\|_{H^2} + \Delta t^{\alpha+1}\|g^n\|_{H^1} \\
&\le C\,\Delta t^{\alpha-1/2}(C_1 + \Delta t^{3/2}\|g^n\|_{H^1}) .
\end{aligned}
\tag{6.86}
$$

Obviously, we have

$$
\|\nabla e^n\| \le \sum_{k=0}^{n} \|\nabla(e^k + e^{k-1})\| \le C_1\,\Delta t^{\alpha-3/2} . \tag{6.87}
$$

From the first equation of (6.69) we obtain

$$
\begin{aligned}
\|\Delta e^*\| &\le \Delta t^{-1}\|e^* - e^n\| + C\,\|e^n\| + \|\nabla e^n\| + C\,\Delta t^\alpha\|f^n\| \\
&\le C_1\Delta t^{\alpha-3/2} .
\end{aligned}
\tag{6.88}
$$

Consequently, we have

$$
\|e^*\|_{H^2} \le C_1\Delta t^{\alpha-3/2} , \qquad \|e^*\|_{L^\infty} \le C_1\Delta t^{\alpha-3/4} . \tag{6.89}
$$

From the second equation of (6.69), we have

$$
\|\nabla(q^{n+1} - q^n)\| \le C_1\Delta t^{\alpha-1} \tag{6.90}
$$

and

$$\begin{aligned} \|\Delta(q^{n+1} - q^n)\|_{H^1} &\le \Delta t^{-1}\|e^*\|_{H^2} + \Delta t^{\alpha}\|g^n\|_{H^2} \\ &\le C\,\Delta t^{\alpha-5/2}(C_1 + \Delta t^2\|g^n\|_{H^2})\,. \end{aligned} \tag{6.91}$$

Hence, we have

$$\|q^{n+1} - q^n\|_{H^3} \le C_1\Delta t^{\alpha-5/2} \tag{6.92}$$

and

$$\|\nabla(q^{n+1} - q^n)\|_{L^\infty} \le C_1\Delta t^{\alpha-7/4}\,. \tag{6.93}$$

Using the second equation of (6.69) once more, we get

$$\begin{aligned} \|e^{n+1} + e^n\|_{L^\infty} &\le \|e^*\|_{L^\infty} + \Delta t\ \|\nabla(q^{n+1} - q^n)\|_{L^\infty} + \Delta t^{\alpha+1}\|g^n\|_{L^\infty} \\ &\le C_1\Delta t^{\alpha-3/4}\,. \end{aligned} \tag{6.94}$$

Hence we have

$$\|e^n\|_{L^\infty} \le C_1\Delta t^{\alpha-7/4}\,. \tag{6.95}$$

As in §4.2, if we choose Δt small enough, we have $\|e^n\|_{L^\infty} \le 1$. Hence in (6.65) we can choose

$$\tilde{C} = 1 + \max_{n\le[\frac{T}{\Delta t}]+1} \|U^n(\cdot)\|_{L^\infty}$$

which depends only on the exact solution $(\boldsymbol{u}, p)$. Combining (6.66), (6.68), and (6.95), we get

$$\|\boldsymbol{u}^n - U^n\|_{L^\infty} + \|\boldsymbol{u}^* - U^*\|_{L^\infty} + \Delta t\|p^n - P^n\|_{W^{1,\infty}} \le C_1\Delta t^{\alpha-7/4}\,. \tag{6.96}$$

This completes the proof of the proposition.

7. Generalizations. Our goal is not to prove the most general theorems possible, but rather to elucidate the numerical phenomena involved. Nevertheless, we will mention here briefly some possibilities of generalizing the main results. The proofs of these statements are more or less straightforward, following the ideas presented above, although the actual details can be very tedious.

(1) There is no difficulty in generalizing Theorems 3.1–3.4 to three-dimensional problems. Only obvious changes are required for the statement of the results and their proofs. This also marks an advantage of the projection method: In going from two to three dimensions, the formulation basically remains the same.

(2) More general spatial discretizations can be considered, such as the spectral method, finite element method, or more general finite difference method. However, one has to be careful in the projection step since it is in the mixed formulation:

$$\begin{cases} \boldsymbol{u}^{n+1} + \Delta t\nabla p^{n+1} = \boldsymbol{u}^*\,, \\ \nabla\cdot\boldsymbol{u}^{n+1} = 0\,, \\ \left.\dfrac{\partial p^{n+1}}{\partial \boldsymbol{n}}\right|_{\partial\Omega} = 0\,. \end{cases} \tag{7.1}$$

The basic stability criteria for mixed problems such as the inf-sup condition has to be satisfied. In other words, the null space of the discrete laplacian for pressure may contain functions other than the constant functions. These so-called "parasitic modes" have to be subtracted to obtain the pressure approximation (see [1]).

(3) More interesting is the generalization to general domains. Obviously the stability and a priori estimates in §§4.2 and 6.2 require no change. The changes required for the asymptotic analysis are described below.

Let $\boldsymbol{x} = \boldsymbol{R}(s) + \varepsilon\rho\boldsymbol{n}$, where $\boldsymbol{R}(s)$ is a point at $\partial\Omega$, s is the arclength of $\partial\Omega$ from a reference point to $\boldsymbol{R}(s)$, and $\boldsymbol{n}$ is the inward normal of $\partial\Omega$ at $\boldsymbol{R}(s)$. We will use (s,ρ) as our coordinates for the boundary layer terms, and denote by $\boldsymbol{e}_s$ and $\boldsymbol{e}_\rho$ the unit coordinate vectors. This is a well-defined coordinate system near the boundary. It is an orthogonal system. The scaling factors h_1 and h_2 are given by

$$h_1 = \left(\frac{\partial \boldsymbol{x}}{\partial s}\cdot\frac{\partial \boldsymbol{x}}{\partial s}\right)^{1/2} = 1 + \varepsilon\rho\kappa(s)\,, \quad h_2 = \left(\frac{\partial \boldsymbol{x}}{\partial \rho}\cdot\frac{\partial \boldsymbol{x}}{\partial \rho}\right)^{1/2} = \varepsilon, \tag{7.2}$$

where κ is the curvature of $\partial\Omega$ at $\boldsymbol{R}(s)$, positive for a convex curve. In this coordinate system, the differential operators take the following form:

$$\Delta u(s,\rho) = \frac{1}{\varepsilon(1+\varepsilon\rho\kappa)}\left[\frac{\partial}{\partial s}\left(\frac{\varepsilon}{1+\varepsilon\rho\kappa}\frac{\partial u}{\partial s}\right) + \frac{\partial}{\partial \rho}\left(\frac{1+\varepsilon\rho\kappa}{\varepsilon}\frac{\partial u}{\partial \rho}\right)\right], \tag{7.3}$$

$$\nabla p = \frac{1}{1+\varepsilon\rho\kappa}\frac{\partial p}{\partial s}\boldsymbol{e}_s + \frac{1}{\varepsilon}\frac{\partial p}{\partial \rho}\boldsymbol{e}_\rho\,, \tag{7.4}$$

$$\nabla\cdot(u\boldsymbol{e}_s + v\boldsymbol{e}_\rho) = \frac{1}{\varepsilon(1+\varepsilon\rho\kappa)}\left\{\varepsilon\frac{\partial u}{\partial s} + \frac{\partial}{\partial \rho}[(1+\varepsilon\rho\kappa)v]\right\}. \tag{7.5}$$

Now we can repeat the analysis in §§4.1 and 6.1 using these formulas. Here we will only outline the necessary changes for the first-order scheme analyzed in §4. The interested reader can fill in the details for the other cases.

The ansatz remains the same as (4.2), with ξ replaced by ρ and y replaced by s in the boundary layer terms. We should keep in mind that (4.2) is only valid near the boundary and the vectors are decomposed using the basis $\{\boldsymbol{e}_s, \boldsymbol{e}_\rho\}$. In the interior of the domain, the numerical solution admits a regular perturbation expansion.

It is easy to see that $\boldsymbol{u}_j^*$, $\boldsymbol{u}_j$, p_j, $j = 0,1,2,\ldots$ still satisfy the same equations as in §4, whereas the equations for the boundary layer terms are changed as follows:

$$\boldsymbol{a}_1^* = 0\,, \tag{7.6}$$

$$\boldsymbol{a}_2^* = \frac{\partial^2 \boldsymbol{a}_2^*}{\partial \rho^2}\,, \quad \boldsymbol{a}_2^* = \frac{\partial \varphi_1}{\partial \rho}\boldsymbol{e}_\rho\,, \tag{7.7}$$

$$\left.\frac{\partial \varphi_1}{\partial \rho}\right|_{\rho=0} = -\left.\frac{\partial p_0}{\partial \boldsymbol{n}}\right|_{\partial\Omega}. \tag{7.8}$$

Therefore we have

$$\varphi_1(\rho,s) = \left.\frac{\partial p_0}{\partial \boldsymbol{n}}\right|_{\partial\Omega} e^{-\rho}\,. \tag{7.9}$$

For $\boldsymbol{a}_3^*$ and φ_2 we have

$$\boldsymbol{a}_3^* = \frac{\partial \varphi_2}{\partial \rho}\boldsymbol{e}_\rho + \frac{\partial \varphi_1}{\partial s}\boldsymbol{e}_s\,, \quad \boldsymbol{a}_3^* = \partial^2 \boldsymbol{a}_3^* \partial \rho^2 + \kappa \frac{\partial \boldsymbol{a}_2^*}{\partial \rho}\,, \tag{7.10}$$

$$\left.\frac{\partial \varphi_2}{\partial \rho}\right|_{\rho=0} = 0\,. \tag{7.11}$$

From (7.10) and (7.11), we get

$$\varphi_2(\rho, s) = \frac{1}{2}\kappa(s)\left.\frac{\partial p_0}{\partial \boldsymbol{n}}\right|_{\partial\Omega}(1+\rho)e^{-\rho}\,. \tag{7.12}$$

We next have

$$\boldsymbol{a}_4^* = \frac{\partial \varphi_3}{\partial \rho}\boldsymbol{e}_\rho + \left(\frac{\partial \varphi_2}{\partial s} - \rho\kappa\frac{\partial \varphi_1}{\partial s}\right)\boldsymbol{e}_s\,, \tag{7.13}$$

$$\boldsymbol{a}_4^* = \frac{\partial^2 \boldsymbol{a}_4^*}{\partial \rho^2} + \kappa\frac{\partial \boldsymbol{a}_3^*}{\partial \rho} - \rho\kappa^2\frac{\partial \boldsymbol{a}_2^*}{\partial \rho} + \frac{\partial^2 \boldsymbol{a}_2^*}{\partial s^2}\,, \tag{7.14}$$

$$\left.\frac{\partial \varphi_3}{\partial \rho}\right|_{\rho=0} = -\left.\frac{\partial p_2}{\partial \boldsymbol{n}}\right|_{\partial\Omega}. \tag{7.15}$$

In a priori, it is not clear whether (7.13) and (7.14) are consistent (which means that we might have to introduce boundary layer terms in $\boldsymbol{u}^n$). But if we write $\boldsymbol{a}_4^* = a_4^*\boldsymbol{e}_\rho + b_4^*\boldsymbol{e}_s$, and use the fact that $\frac{\partial \boldsymbol{e}_s}{\partial s} = \kappa\boldsymbol{e}_\rho$, $\frac{\partial \boldsymbol{e}_\rho}{\partial s} = -\kappa\boldsymbol{e}_s$, we see that (7.14) is equivalent to

$$a_4^* = \frac{\partial^2 a_4^*}{\partial \rho^2} + \kappa\frac{\partial^2 \varphi_2}{\partial \rho^2} - \rho\kappa^2\frac{\partial^2 \varphi_1}{\partial \rho^2} + \frac{\partial^3 \varphi_1}{\partial \rho \partial s^2} - \kappa^2\frac{\partial \varphi_1}{\partial \rho}\,, \tag{7.16}$$

$$b_4^* = \frac{\partial^2 b_4^*}{\partial \rho^2} + 2\kappa\frac{\partial^2 \varphi_1}{\partial \rho \partial s} + \frac{\partial}{\partial s}\left(\kappa\frac{\partial \varphi_1}{\partial \rho}\right). \tag{7.17}$$

(7.16) serves as the equation for φ_3, together with the boundary condition (7.15). (7.17) is satisfied by $b_4^* = \frac{\partial \varphi_2}{\partial s} - \rho\kappa\frac{\partial \varphi_1}{\partial s}$. This procedure can obviously be continued to as high order as we wish.

In summary, we obtain the following extension of Theorem 3.1.

THEOREM 7.1. *Let $(\boldsymbol{u}, p)$ be a smooth solution of the Navier–Stokes equation* (2.1) *with smooth initial data $\boldsymbol{u}^0(\boldsymbol{x})$ and let $(\boldsymbol{u}_{\triangle t}, p_{\triangle t})$ be the numerical solution for the semidiscrete projection method* (2.6), (2.7), *and* (2.10). *Then we have*

$$\|\boldsymbol{u} - \boldsymbol{u}_{\triangle t}\|_{L^\infty(0,T;L^2)} + \triangle t^{1/2}\|p - p_{\triangle t}\|_{L^2(0,T;L^2)} \le C\triangle t\,. \tag{7.18}$$

Furthermore, if $\boldsymbol{u}^0(\boldsymbol{x})$ satisfies the compatibility condition

$$\boldsymbol{u}^0(\boldsymbol{x}) = 0\,, \quad \frac{\partial p}{\partial \boldsymbol{n}}(\boldsymbol{x}, 0) = 0 \quad \text{on } \partial\Omega\,, \tag{7.19}$$

then we have

$$\|\boldsymbol{u}-\boldsymbol{u}_{\triangle t}\|_{L^\infty}+\triangle t^{1/2}\,\|p-p_{\triangle t}\|_{L^\infty}+\|p-p_{\triangle t}-p_c\|_{L^\infty}\le C\triangle t \tag{7.20}$$

where

$$p_c(\boldsymbol{x},t)=\triangle t^{1/2}\frac{e}{e-1}e^{-\rho}\frac{\partial p_{\triangle t}}{\partial \boldsymbol{n}}(s,\rho+\triangle t^{1/2},t)\,.$$

The required change for the extension of Theorem 3.2 to general domains is more or less the same.

(4) One can also consider the generalization to other types of boundary conditions, including inhomogeneous ones.

Appendix 1. Postprocessing for the pressure. Theorem 3.2 tells us how to correct the leading-order boundary layer error in the numerical approximations of pressure. Here we will show how the next order boundary layer terms can also be corrected. The asymptotic analysis in §6.2 gives

$$p_{\triangle t}=p_0+\varepsilon\phi_1+\varepsilon^3\phi_3+O(\triangle t^2) \tag{8.1}$$

where

$$\phi_1=\frac{1}{\sqrt{2}}e^{-\sqrt{2}\xi}\,\partial_x p_0\,|_{x=-1}, \tag{8.2}$$

$$\phi_3=\frac{1}{2}\left(\frac{1}{\sqrt{2}}+\xi\right)e^{-\sqrt{2}\xi}\,\partial_{xyy}p_0\,|_{x=-1}\,. \tag{8.3}$$

All these and the following formulas are evaluated at $(n-\frac{1}{2})\triangle t$. From (8.1) we have

$$\begin{aligned}\partial_x p_{\triangle t}\,|_{x=-1+\triangle t^{1/2}} &= \partial_x p_0\,|_{x=-1+\triangle t^{1/2}}-e^{-\sqrt{2}}\partial_x p_0\,|_{x=-1}\\ &\quad -\frac{\triangle t}{\sqrt{2}}e^{-\sqrt{2}}\partial_{xyy}p_0\,|_{x=-1}+O(\triangle t^{3/2}).\end{aligned} \tag{8.4}$$

Hence we have

$$\partial_{xyy}p_0\,|_{x=-1}=\frac{e^{\sqrt{2}}}{e^{\sqrt{2}}-1}\partial_{xyy}p_{\triangle t}\,|_{x=-1+\triangle t^{1/2}}+O(\triangle t^{1/2}). \tag{8.5}$$

Taylor expansion gives

$$\begin{aligned}\partial_x p_0\,|_{x=-1+\triangle t^{1/2}} &= \partial_x p_0\,|_{x=-1}-\varepsilon\partial_x^2 p_0\,|_{x=-1+\triangle t^{1/2}}\\ &\quad -\frac{\varepsilon^2}{2}\partial_x^3 p_0\,|_{x=-1+\triangle t^{1/2}}+O(\triangle t^{3/2}).\end{aligned} \tag{8.6}$$

Again from (8.1) we have

$$\begin{aligned}\varepsilon\partial_x^2 p_{\triangle t} &= \varepsilon\partial_x^2 p_0+\partial_\xi^2\phi_1+\varepsilon^2\partial_\xi^2\phi_3+O(\triangle t^{3/2})\\ &= \varepsilon\partial_x^2 p_0+\sqrt{2}e^{-\sqrt{2}\xi}\,\partial_x p_0\,|_{x=-1}\\ &\quad +\varepsilon^2\left(\xi-\frac{1}{\sqrt{2}}\right)e^{-\sqrt{2}\xi}\,\partial_{xyy}p_0\,|_{x=-1}+O(\triangle t^{3/2}),\end{aligned} \tag{8.7}$$

$$
\begin{aligned}
\frac{\varepsilon^2}{2}\partial_x^3 p_{\triangle t} &= \frac{\varepsilon^2}{2}\partial_x^3 p_0 + \frac{1}{2}\partial_\xi^3\phi_1 + \frac{\varepsilon^2}{2}\partial_\xi^3\phi_3 + O(\triangle t^{3/2}) \\
&= \frac{\varepsilon^2}{2}\partial_x^3 p_0 - e^{-\sqrt{2}\xi}\,\partial_x p_0\,|_{x=-1} \\
&\quad +\varepsilon^2\left(1-\frac{\xi}{\sqrt{2}}\right)e^{-\sqrt{2}\xi}\,\partial_{xyy}p_0\,|_{x=-1} + O(\triangle t^{3/2}).
\end{aligned} \tag{8.8}
$$

Evaluating these expressions at $x = -1 + \triangle t^{1/2}$, we get

$$
\begin{aligned}
\varepsilon\partial_x^2 p_{\triangle t}\,|_{x=-1+\triangle t^{1/2}} &= \varepsilon\partial_x^2 p_0\,|_{x=-1+\triangle t^{1/2}} + \sqrt{2}e^{-\sqrt{2}}\partial_x p_0\,|_{x=-1} \\
&\quad +\varepsilon^2\left(1-\frac{1}{\sqrt{2}}\right)e^{-\sqrt{2}}\partial_{xyy}p_0\,|_{x=-1} + O(\triangle t^{3/2}),
\end{aligned} \tag{8.9}
$$

$$
\begin{aligned}
\frac{\varepsilon^2}{2}\partial_x^3 p_{\triangle t}\,|_{x=-1+\triangle t^{1/2}} &= \frac{\varepsilon^2}{2}\partial_x^3 p_0\,|_{x=-1+\triangle t^{1/2}} - e^{-\sqrt{2}}\,\partial_x p_0\,|_{x=-1} \\
&\quad +\varepsilon^2\left(1-\frac{1}{\sqrt{2}}\right)e^{-\sqrt{2}}\,\partial_{xyy}p_0\,|_{x=-1} + O(\triangle t^{3/2}).
\end{aligned} \tag{8.10}
$$

Combining (8.4), (8.6), (8.9), and (8.10), we obtain

$$
\begin{aligned}
&\left(\partial_x + \varepsilon\partial_x^2 + \frac{\varepsilon^2}{2}\partial_x^3\right)p_{\triangle t}\,|_{x=-1+\triangle t^{1/2}} = [1-(2-\sqrt{2})e^{-\sqrt{2}}]\partial_x p_0\,|_{x=-1} \\
&\qquad +\triangle t\frac{2\sqrt{2}-3}{\sqrt{2}}e^{-\sqrt{2}}\,\partial_{xyy}p_0\,|_{x=-1} + O(\triangle t^{3/2}).
\end{aligned} \tag{8.11}
$$

Or

$$
\begin{aligned}
\partial_x p_0\,|_{x=-1} &= \frac{e^{\sqrt{2}}}{e^{\sqrt{2}}-2+\sqrt{2}}\left(\partial_x + \varepsilon\partial_x^2 + \frac{\varepsilon^2}{2}\partial_x^3\right)p_{\triangle t}\,|_{x=-1+\triangle t^{1/2}} \\
&\quad -\triangle t\frac{2\sqrt{2}-3}{\sqrt{2}e^{\sqrt{2}}+2-3\sqrt{2}+2(\sqrt{2}-1)e^{-\sqrt{2}}}\,\partial_{xyy}p_{\triangle t}\,|_{x=-1+\triangle t^{1/2}} \\
&\quad +O(\triangle t^{3/2}).
\end{aligned} \tag{8.12}
$$

Finally, using (8.5) and (8.12) in (8.1), (8.2), and (8.3), we get

$$
p_{\triangle t} = p_0 - p_c + O(\triangle t^2) \tag{8.13}
$$

where

$$
\begin{aligned}
p_c &= \alpha\triangle t^{1/2}e^{-\sqrt{2}\xi}\left(\partial_x + \triangle t^{1/2}\partial_x^2 + \frac{\triangle t}{2}\partial_x^3\right)p_{\triangle t}\,|_{x=-1+\triangle t^{1/2}} \\
&\quad +(\beta+\gamma\xi)\triangle t^{3/2}e^{-\sqrt{2}\xi}\,\partial_{xyy}p_{\triangle t}\,|_{x=-1+\triangle t^{1/2}},
\end{aligned} \tag{8.14}
$$

where

$$
\begin{aligned}
\alpha &= \frac{e^{\sqrt{2}}}{2-2\sqrt{2}+\sqrt{2}e^{\sqrt{2}}}, \\
\beta &= \frac{1}{2\sqrt{2}}\frac{e^{\sqrt{2}}}{2e^{\sqrt{2}}-2} - \frac{2\sqrt{2}-3}{\sqrt{2}e^{\sqrt{2}}+2-3\sqrt{2}+2(\sqrt{2}-1)e^{-\sqrt{2}}}, \\
\gamma &= \frac{e^{\sqrt{2}}}{2e^{\sqrt{2}}-2}.
\end{aligned} \tag{8.15}
$$

Acknowledgments. We are very grateful to Alexandre Chorin for bringing this problem to our attention and for numerous stimulating discussions. We also want to thank Tom Beale for communicating to us other related work.

REFERENCES

[1] C. R. ANDERSON, *Derivation and solution of the discrete pressure equations for the incompressible Navier–Stokes equations*, manuscript.

[2] T. BEALE AND C. GREENGARD, *Convergence of Euler–Stokes splitting of the Navier–Stokes equations*, preprint.

[3] J. B. BELL, P. COLELLA, AND H. M. GLAZ, *A second-order projection method for the incompressible Navier–Stokes equations,* J. Comput. Phys., 85 (1989), pp. 257–283.

[4] J. B. BELL AND D. MARCUS, *A second-order projection method for variable-density flows,* J. Comput. Phys., 101 (1992), pp. 334–348.

[5] A. J. CHORIN, *The numerical solution of the Navier–Stokes equations for an incompressible fluid,* Bull. Amer. Math. Soc., 73 (1967), pp. 928–931.

[6] ———, *Numerical solution of the Navier-Stokes equations,* Math. Comp., 22 (1968), pp. 745–762.

[7] ———, *On the convergence of discrete approximations to the Navier–Stokes equations,* Math. Comp., 23 (1969), pp. 341–353.

[8] ———, *Computational Fluid Mechanics, Selected Papers,* Academic Press, New York, 1989.

[9] WEINAN E AND J.-G. LIU, *Projection method* II: *Rigorous Godunov–Ryabenki analysis*, SIAM J. Numer. Anal., to appear.

[10] ———, *Projection method with spatial discretizations*, manuscript, 1992.

[11] P. M. GRESHO, *Incompressible fluid dynamics: Some fundamental formulation issues,* Ann. Rev. Fluid Mech., 23 (1991), pp. 413–453.

[12] ———, *Some interesting issues in incompressible fluid dynamics, both in the continuum and in numerical simulation,* Adv. Appl. Mech., 28 (1992), pp. 45–139.

[13] J.-L. GUERMOND, *Remarques sur les methodes de projection pour l'approximation des equations de Navier–Stokes*, Numer. Math., 67 (1994), pp. 465–473.

[14] J. HEYWOOD AND R. RANNACHER, *Finite element approximation of the nonstationary Navier–Stokes problem, part* III. *Smoothing property and higher order error estimates for spatial discretization*, SIAM J. Numer. Anal., 25 (1988), pp. 490–512.

[15] G. KARNIADAKIS, M. ISRAELI, AND S. A. ORSZAG, *High-order splitting methods for the incompressible Navier–Stokes equations,* J. Comput. Phys., 97 (1991), pp. 414–443.

[16] J. KIM AND P. MOIN, *Application of a fractional-step method to incompressible Navier–Stokes equations,* J. Comput. Phys., 59 (1985), pp. 308–323.

[17] D. MICHELSON, *Convergence theorems for finite difference approximations for hyperbolic quasilinear initial-boundary value problems*, Math. Comp., 49 (1987), pp. 445–459.

[18] H. OKAMOTO, *On the semi-discrete finite element approximation for the nonstationary Navier–Stokes equation*, J. Fac. Sci. Univ. Tokyo Sect. IA Math., 29 (1982), pp. 612–652.

[19] S. A. ORSZAG, M. ISRAELI, AND M. O. DEVILLE, *Boundary conditions for incompressible flows,* J. Sci. Comput., 1 (1986), pp. 75–111.

[20] M. M. RAI AND P. MOIN, *Direct simulation of turbulent flow using finite-difference schemes,* J. Comput. Phys., 96 (1991), pp. 15–53.

[21] R. RANNACHER, *On Chorin's projection method for the incompressible Navier–Stokes equations,* Lecture Notes in Mathematics, 1530 (1992), pp. 167–183.

[22] J. SHEN, *On error estimates of projection methods for Navier–Stokes equations: First order schemes,* SIAM J. Numer. Anal., 29 (1992), pp. 57–77.

[23] ———, *On error estimates of some higher order projection and penalty-projection methods for Navier–Stokes equations,* Numer. Math., 62 (1992), pp. 49–73.

[24] G. STRANG, *Accurate partial difference methods* II. *Non-linear problems,* Numer. Math., 6 (1964), pp. 37–46.

[25] R. TEMAM, *Sur l'approximation de la solution des equations de Navier–Stokes par la méthode des fractionnarires* II, Arch. Rational Mech. Anal., 33 (1969), pp. 377–385.

[26] ———, *Navier Stokes Equations,* North Holland, New York, 1977.

[27] ———, *Remark on the pressure boundary condition for the projection method,* Theoret. Computational Fluid Dynamics, 3 (1991), pp. 181–184.

[28] J. VAN KAN, *A second-order accurate pressure-correction scheme for viscous incompressible flow,* SIAM J. Sci. Statist. Comp., 7 (1986), pp. 870–891.